A role for seipin in lipid droplet dynamics and inheritance in yeast

Heimo Wolinski[1], Dagmar Kolb[1,*], Sandra Hermann[1], Roman I. Koning[2] and Sepp D. Kohlwein[1,‡]

[1]Institute of Molecular Biosciences, University of Graz, Humboldtstr. 50/II, 8010 Graz, Austria
[2]Leiden University Medical Center, Department of Molecular Cell Biology, Leiden, The Netherlands

*Present address: Institute of Histology, Medical University Graz, 8010 Graz, Austria
‡Author for correspondence (sepp.kohlwein@uni-graz.at)

Accepted 4 July 2011
Journal of Cell Science 124, 3894–3904

doi: 10.1242/jcs.091454

Summary

Malfunctions of processes involved in cellular lipid storage and mobilization induce the pathogenesis of prevalent human diseases such as obesity, type 2 diabetes and atherosclerosis. Lipid droplets are the main lipid storage depots for neutral lipids in eukaryotic cells, and as such fulfil an essential function to balance cellular lipid metabolism and energy homeostasis. Despite significant progress in identifying key metabolic enzymes involved in lipid storage and their regulation in various model organisms, some fundamental questions as to the biogenesis, subcellular distribution and inheritance of lipid droplets are as yet unsolved. In this study, we applied a set of imaging techniques such as high-resolution four-dimensional (4D) live-cell imaging, quantitative microscopy, transmission electron microscopy and electron tomography to gain insight into the spatio-temporal organization of lipid droplets during cellular growth in the yeast *Saccharomyces cerevisiae*. This analysis revealed a high level of organization of the subcellular positioning of lipid droplets in individual cells, their directed migration towards the cellular periphery and a coordinated transfer of a subpopulation of lipid droplets into daughter cells during cell division. Lipid droplets appear to remain associated with ER membranes during cellular growth independently of their size and subcellular localization. Deletion of *FLD1*, the functional orthologue of the human *BSCL2* gene encoding seipin, leads to impaired dynamics of yeast lipid droplets and defective lipolysis, which might be due to aberrant ER structures in these mutants. Our data suggest a role for yeast seipin as a scaffolding protein that is required for the dynamics of a specific subdomain of the ER, and provide a new aspect for the interpretation of abnormal lipid droplets phenotypes in yeast mutants lacking seipin.

Key words: Neutral lipid, Lipolysis, Lipid droplet, Endoplasmic reticulum, Fluorescence microscopy, Electron microscopy, Tomography, *Saccharomyces cerevisiae*

Introduction

Lipid droplets form the main lipid storage organelles for neutral lipids in eukaryotic cells. The hydrophobic core of lipid droplets consists predominantly of the neutral lipids, triacylglycerols (TAGs) and steryl esters (SEs). Lipid droplets are surrounded by a phospholipid monolayer, which contains a subset of proteins catalyzing the synthesis or mobilization of neutral lipids. The composition of lipid droplets and the molecular and regulatory mechanisms of stockpiling of lipids is highly conserved among eukaryotic cells (Farese and Walther, 2009; Martin and Parton, 2006). Lipid droplets are essential organelles for balanced cellular lipid metabolism and energy homeostasis. In mammals, dysregulation or dysfunction of these processes causes highly prevalent metabolic diseases such as obesity, type-2 diabetes and atherosclerosis. In addition, the organelle also participates in a range of other functions such as cell signaling or intracellular vesicle trafficking (Liu et al., 2007). In this respect, lipid droplets have been recognized as metabolically highly active organelles. Owing to the importance of lipid droplets for vital functions, the organelle, its associated proteins and interaction with other organelles are subject of extensive investigations in different model systems including the yeast *Saccharomyces cerevisiae* (Athenstaedt and Daum, 2006; Daum et al., 2007; Goodman, 2008; Sturley, 2000).

In recent years, a variety of molecular and biochemical details of neutral lipid metabolism have been revealed. However, cell biological aspects of lipid droplets such as their biogenesis, the mode of degradation, regulatory mechanisms and their interactions with other organelles remain largely elusive, both in mammalian and non-mammalian cell systems. In this context, the motility and positioning of lipid droplets during cell differentiation and cellular growth, respectively, is an emerging issue. In many cells, lipid droplets seem to undergo active motion, typically along microtubules, even though the physiological role of the intracellular movement of lipid droplets is still speculative (Welte, 2009). However, the subcellular distribution of lipid droplets and their morphology in distinct stages of cell development has been discussed as an important factor for the identification of malfunctions in neutral lipid homeostasis. Thus, imaging-based phenotypic screens in different model systems such as *Drosophila melanogaster* (Beller et al., 2008; Guo et al., 2008), *Caenorhabditis elegans* (Ashrafi et al., 2003) and the yeast *Saccharomyces cerevisiae* (Fei et al., 2008b; Szymanski et al., 2007) have been applied to reveal protein candidates that affect lipid droplet phenotypes.

The yeast *FLD1* gene was recently identified by two independent studies as the functional orthologue of the human *BSCL2* gene (Fei et al., 2008b; Szymanski et al., 2007). *BSCL2*

encodes seipin, a protein with an unknown function; mutations in *BSCL2* cause the more severe recessive inherited form of lipodystrophy, Berardinelli–Seip congenital lipodystrophy Type 2. Patients affected by this disease lack adipose tissue, which might be caused by a malfunction in the differentiation of mesenchymal cells into preadipocytes (Agarwal and Garg, 2004). In addition, they are hyperphagic, which leads to fat accumulation in liver and muscles, and they frequently acquire insulin resistance and diabetes similarly to obese patients. Patients often die at an early age as a result of liver failure (Garg, 2004; Simha and Garg, 2009). Mutations in the *BSCL2* gene can also be inherited dominantly: such mutations in the glycosylation site of BSCL2 cause several motor neuron diseases such as Silver syndrome (Windpassinger et al., 2004). In these cells, mutant seipin activates unfolded protein response (UPR) stress and induces ER-stress-mediated apoptosis. It was therefore suggested that these diseases are tightly associated with ER-stress-mediated cell death (Ito and Suzuki, 2007).

Interestingly, in yeast, the deletion of *FLD1* causes different lipid droplet phenotypes. Cell populations of the *fld1* mutant strain either contain 'super-sized' lipid droplets or a number of irregular lipid droplets that appear often clustered alongside proliferated ER structures. It was suggested that the generation of super-sized lipid droplets in the *fld1* strain is caused by a change of the phospholipid composition of the membrane monolayer of the organelle (Fei et al., 2008b). By contrast, the occurrence of irregular, 'chaotic budding' of lipid droplets and the localization of Fld1 at lipid droplets to ER interfaces indicate a structural function of Fld1 in organizing lipid droplets or in the interaction between lipid droplets and the ER (Binns et al., 2010; Szymanski et al., 2007).

In the present study, we provide evidence for an additional role for yeast seipin. In wild-type cells, we show that the spatial subcellular positioning of lipid droplets in individual cells follows a specific dynamic distribution pattern, over several cell generations. In these cells, two subpopulations of lipid droplets exist; they differ in their dynamic behavior, of which one fraction is inherited into daughter cells, whereas another fraction moves towards the cellular periphery in the mother cells. Lack of Fld1 causes impaired inheritance and degradation of lipid droplets. We discuss the appearance of 'immobile' ER structures as a factor causing abnormal dynamic behavior of lipid droplets in the *fld1* deletion mutant strain, and suggest a function of yeast Fld1 as a scaffolding protein required for regular dynamics of a specific domain of the ER.

Results

The dynamic spatial distribution of lipid droplets in growing cells

The subcellular distribution of lipid droplets in yeast follows a specific pattern during cellular growth. Thus, we set out to apply high-resolution time-lapsed three-dimensional live-cell imaging (4D imaging) to study the subcellular positioning and morphological alterations of lipid droplets in growing cells. Yeast cells were cultivated for 5 days in rich medium to the stationary growth phase, which leads to the accumulation of fat in lipid droplets. Subsequently, the cells were stained with BODIPY 493/503, mounted on a solid agar sheet containing rich medium, and cultivated directly on the microscope stage for several hours, as described in the Materials and Methods. Supplementation of stationary phase yeast cells with fresh nutrients induces resumption of cellular growth, which causes a rapid degradation of the neutral lipid stores (Kurat et al., 2006). Thus, the 4D experiment was performed under lipolytic growth conditions. To ensure continuous labeling of lipid droplets during cellular growth and to avoid a potential depletion of BODIPY 493/503 from cells by pleiotropic drug-resistance pumps (Wolinski et al., 2009), cell cultivation was performed in the presence of the fluorescence dye. Because neutral lipids and thus lipid droplets might also be formed de novo under the experimental conditions (Zanghellini et al., 2008), cells were additionally treated with cerulenin to block de novo fatty acid synthesis and the accumulation of TAG and SE. Use of this inhibitor thus allows it to faithfully monitor the distribution of already existing lipid droplets without being obscured by the (rapid) formation of new lipid droplets. Yeast cells were imaged three-dimensionally immediately after mounting the cells on the solid medium sheet, after 20 minutes and 1 hour, and subsequently in shorter time intervals of 10 minutes each, up to 4 hours. A final image stack was acquired after 6 hours.

After 6 hours of cultivation, the second daughter cell generation started to form buds, indicating that the fluorescence dye, cerulenin treatment or the preparation conditions did not significantly impair cellular growth. After that time, most cells showed no or only a very small number of minute residual lipid droplets, consistent with biochemical analyses that showed almost complete neutral lipid breakdown under these conditions (Kurat et al., 2006). After 6 hours of cerulenin treatment, several cells showed signs of significant damage, which is expected to be due to the lack of a lipid source after depletion of the neutral lipid stores in the cell. Three representative cells of comparable size were cropped from 4D image data sets and further analyzed (supplementary material Fig. S1).

The subcellular positioning and inheritance of lipid droplets is temporally and spatially highly organized

Yeast cells cultivated to stationary growth phase contain large lipid droplets of relatively homogeneous size (~0.2–0.3 μm in diameter). In individual cells, lipid droplets are spatially concentrated near the nuclear endoplasmic reticulum (nER) (Fig. 1a; supplementary material Movie 1). At 20 minutes after supplementation with fresh nutrients, very small lipid droplets were detectable in unbudded mother cells. Such lipid droplets were frequently positioned towards the cellular periphery (Fig. 1b). Small lipid droplets but also larger lipid droplets close to the cellular periphery were observed both in mother and daughter cells throughout the entire first round of cell division. One hour after mounting the cells on the solid medium sheet first small buds were detectable, and immediately, one or two lipid droplets were transferred into the emerging buds (Fig. 1c). With increasing bud size, there was a corresponding increase in the number of lipid droplets in the developing daughter cells (Fig. 1d), leading to a slightly biased distribution of the existing lipid droplet pool between mother and daughter cells in the absence of lipid de novo synthesis (Fig. 1e). Quantitative analysis of lipid droplets showed that the amount of neutral lipids in daughter cells is ~60–70% of that in the mother cells, indicating that only 30–35% of pre-existing lipid droplets were transferred into the daughter cells (supplementary material Fig. S2). This further demonstrates that lipid droplet inheritance is not simply a random process that should lead to equilibrium of the lipid droplets content between mother and daughter cells.

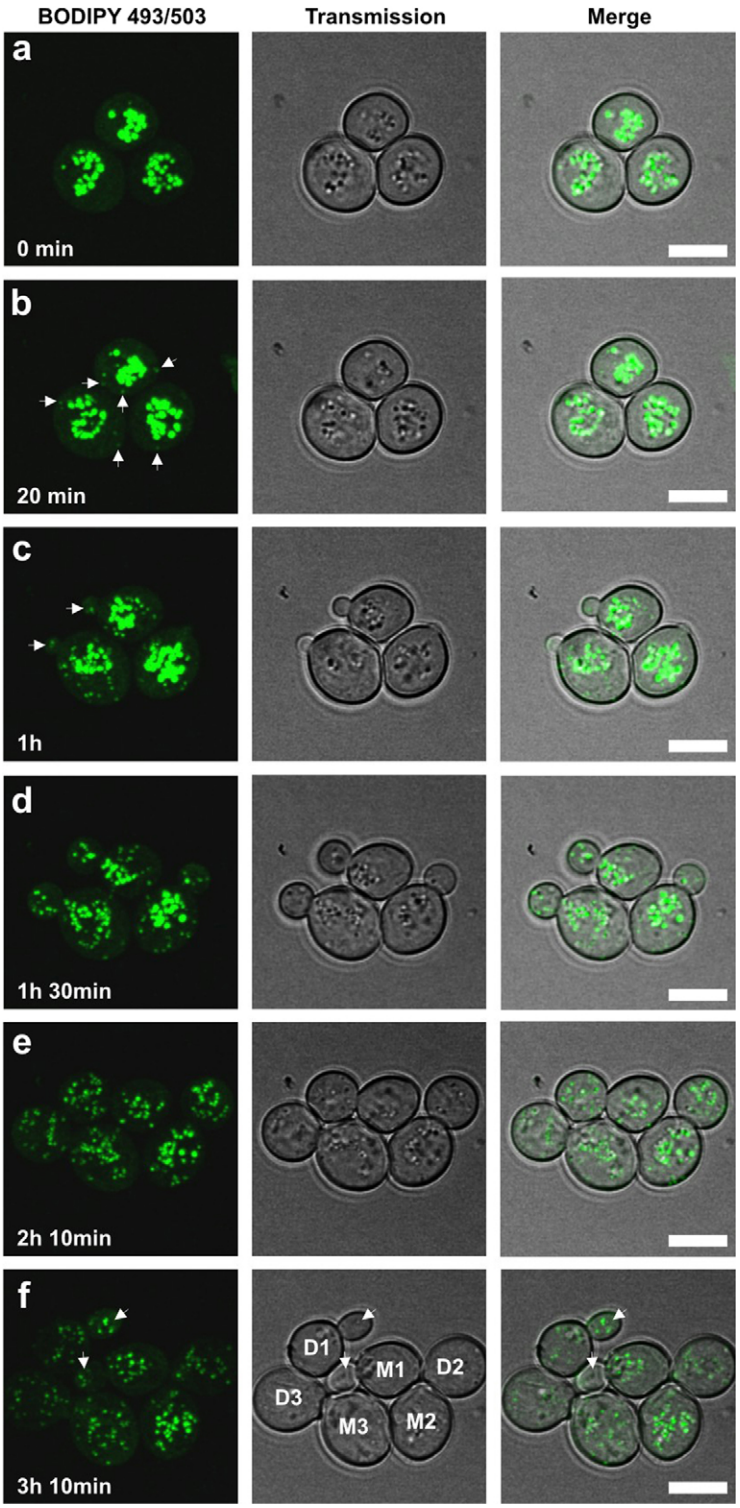

Fig. 1. Subcellular positioning and inheritance of yeast lipid droplets during cellular growth. (**a**) Accumulated lipid droplets of homogeneous size in cells cultivated to stationary growth phase. (**b**) Small lipid droplets orientate towards the cellular periphery in unbudded cells (arrows). (**c**) One or two lipid droplets or lipid droplets 'packages' appear in emerging buds (arrows). (**d**) Lipid droplets in medium-sized buds. (**e**) Lipid droplets in large budded cells. (**f**) Inheritance of lipid droplets into buds of the second cell generation (arrows). Mother cells are labelled as M1–M3, and their corresponding daughter cells as D1–D3. Fluorescence images represent maximum-intensity projections. Transmission images represent single optical sections. Scale bar: 5 μm.

Inheritance of lipid droplets to daughter cells was also observed in the second cell generation, consistent with a specific and regulated inheritance pattern for a subpopulation of the existing lipid droplets pool into newly forming buds (Fig. 1f). Notably, lipid droplets inheritance was independent of the pre-culture conditions (5 days versus 2 days), despite the presence of larger lipid droplets in 5-day stationary phase cells.

To test whether intracellular movement and lipid droplet degradation was dependent on the cytoskeleton, cells were treated with nocodazol (Kunkel, 1980) or latrunculin A (Ayscough et al., 1997) (supplementary material Fig. S3). In the presence of the microtubule-destabilizing drug Nocodazol, lipid droplet inheritance into the daughter cell and lipolysis were not affected. Degradation of the actin cytoskeleton disrupted cell

budding in most cells and lipid droplet inheritance, but lipid droplet degradation was not impaired. These data suggest that movement of lipid droplets is actin dependent, which might result from their close association with the ER membrane and is inherited in an actin-dependent manner (Estrada et al., 2003). Whether lipid droplets directly interact with the actin skeleton is currently unclear.

In summary, we identified two modes of lipid droplets motility in dividing yeast cells: (1) inheritance of a subpopulation of lipid droplets into daughter cells, and (2) movement of lipid droplets from a more central position near the nucleus towards the cellular periphery after stimulation of lipolysis upon addition of nutrients (Kurat et al., 2006), both in mother and daughter cells (supplementary material Fig. S4A,B).

To provide further evidence for a temporally and spatially coordinated inheritance of lipid droplets, we determined the number of lipid droplets in buds of different sizes of a non-synchronized cell culture. We found that the number of lipid droplets was indeed correlated with the bud size (Fig. 2). Thus, we next acquired a 4D image series in 10 minute time intervals to study the transfer of lipid droplets into buds in greater detail. The resulting 4D image series revealed an ordered and sequential transfer of lipid droplets into the growing bud: during that process lipid droplets of the mother cell are located distinctly apart from the bud site and do not accumulate at the bud neck. Thus, delivery of lipid droplets into the daughter cells is clearly a directed process and does not appear to be caused by lipid droplets accumulation at the bud neck and random transfer (supplementary material Fig. S5). To exclude the possibility that appearance of lipid droplets in the daughter cell is due to a disassembly or re-assembly process at the bud neck we traced lipid droplets movement in 300 msecond time intervals (supplementary material Movie 2). This experiment clearly demonstrates that lipid droplets are delivered as a whole into the emerging daughter cell and that this inheritance process does not require prior fragmentation and de novo lipid droplet formation.

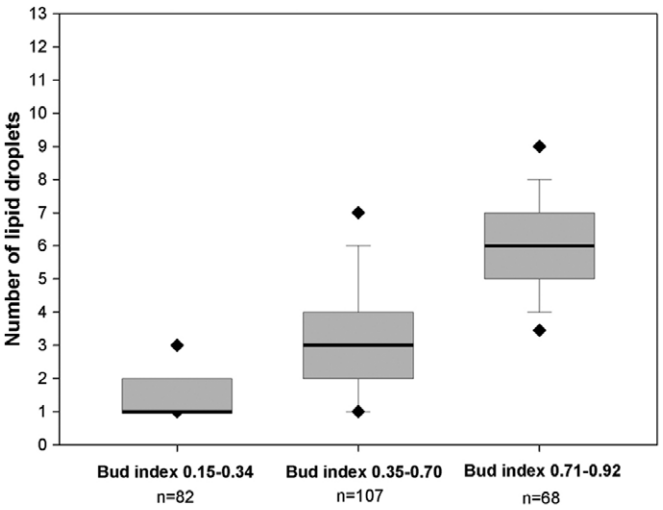

Fig. 2. Imaging-based quantitative analysis of the number of lipid droplets in buds of different sizes in wild-type cells. Three bud categories are defined (small buds, bud index 0.15–0.34; medium-sized buds, bud index 0.35–0.70 and large buds, bud index 0.71–0.92). The box plots show that the number of lipid droplets in a bud is correlated with its size. The number of lipid droplets in small buds is constant. The diamond symbols indicate outliers. Bold lines in the box plots indicate computed median values. At least 200 cells were analyzed.

Because these experiments were performed in the presence of cerulenin to block de novo lipid droplet formation, we next investigated whether these cultivation conditions affected the inheritance pattern of lipid droplets. Also, we wanted to investigate whether de novo lipid droplet formation occurs in both mother and daughter cells or is perhaps confined to one or the other cell type. For this analysis, yeast cells were pre-cultivated to early stationary phase (24 hours) in rich medium and re-inoculated into fresh rich medium without cerulenin. After cultivation for 90 minutes, cells were post-labelled with BODIPY 493/503. A similar mode of lipid droplet positioning and inheritance was observed to that seen in cerulenin-treated cells, in addition to the appearance of a number of small lipid droplets in both mother and daughter cells. These data indicate that the preparation conditions and the growth stage of the cells did not significantly affect the motility and mode of lipid droplets inheritance, and that this dynamic behavior was also independent of de novo lipid droplet formation (supplementary material Fig. S6).

Lipid droplets remain closely associated with ER membranes during cellular growth and lipolysis

Because lipid droplets are transferred into the emerging bud at a very early stage, we next investigated whether this transfer occurred in coordination with ER membranes, to which they appear to be closely attached (Perktold et al., 2007; Szymanski et al., 2007). Wild-type cells harboring the chromosomally integrated ER marker Elo3–GFP were co-labelled with Nile Red to visualize lipid droplets (Greenspan et al., 1985; Wolinski and Kohlwein, 2008). Analysis of 50 imaged cells shows that all detected lipid droplets were – at the level of microscopic resolution – in close association with ER membranes, independently of their size, subcellular position or growth stage (supplementary material Fig. S7, Movie 3). Lipid droplets that are delivered to the emerging bud are also associated with membrane tubules that extend from the bud tip towards the mother cell, and which are presumably contiguous with the ER membrane emanating from the nuclear ER of the mother cell (Fehrenbacher et al., 2002) (Fig. 3).

To obtain a better three-dimensional understanding of the interactions of lipid droplets with the ER in the developing bud, we first applied serial sectioning transmission electron microscopy (3D TEM) covering approximately half of a bud and one third of a mother cell (supplementary material Fig. S8A–C). In accordance with data obtained with fluorescence microscopy, lipid droplets in the small bud always appeared closely associated with the ER membrane extending from the mother cell to the bud tip (Fig. 4a,b). Interactions of lipid droplets with ER membrane were found to be independent of the lipid droplet size (Fig. 4c,d) and always appeared as an ‘egg-in-a-cup’-like arrangement (Fig. 5a–d), as also observed in mammalian cells (Robenek et al., 2006). Interestingly, in our (as well as in many published) electron micrograph, we observed an as yet undefined structure close to the nucleus, which appears to consist of several compartments and a more electron dense matrix. This membrane-surrounded structure contains a number of lipid droplets, and several membrane tubules with associated lipid droplets appear to extend from this subcellular compartment

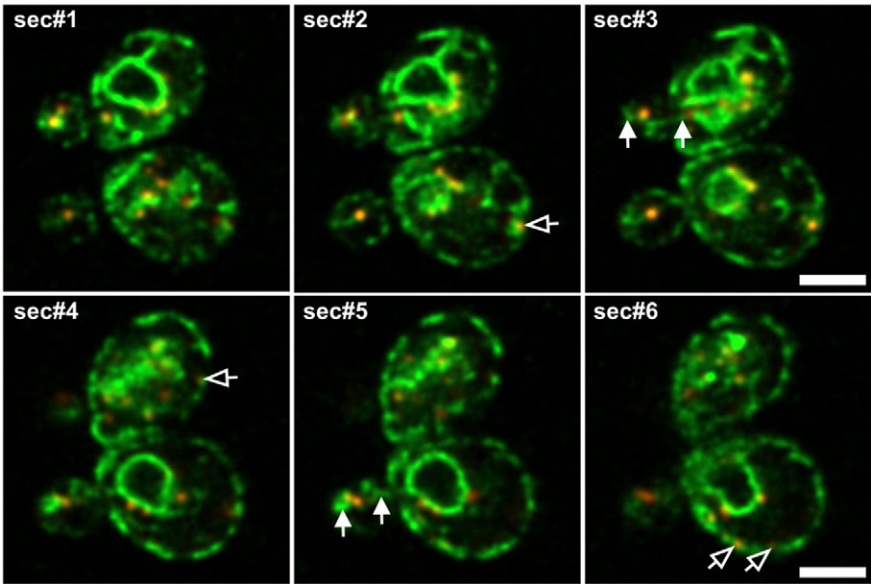

Fig. 3. Association of lipid droplets with ER membranes in small buds. High-resolution images of Elo3–GFP-labelled ER (green) and Nile-Red-labelled lipid droplets (red). Six slices cropped from a 3D dataset are shown. In both cells, lipid droplets in smaller buds are closely associated with an ER extension, reaching from the bud tip towards the mother cell (filled arrows). The nuclei are still not segregated. Both, in the bud and in the mother cell all lipid droplets are associated with ER membranes. Several lipid droplets are visible in close proximity to the cellular periphery (open arrows). Scale bars: 3 μm.

(supplementary material Fig. S8C). Because cells were grown in complete medium and do not suffer from amino acid or other starvation conditions, it is unlikely that these structures resemble autophagosomes; however, the nature of this structure and its potential role in lipid droplets homeostasis are currently under further study.

To provide further proof of a tight association of lipid droplets with ER membranes, we used electron tomography. The selected tomogram shows a representative 'adult' lipid droplets of ~100 nm and its association with the ER membrane. As also observed in the 3D TEM series, this lipid droplet is embedded in a crescent-shaped ER structure (Fig. 6). At this level of resolution, however, it remains unclear whether the ER membrane indeed forms a continuum with the lipid droplet half membrane. Nevertheless, these analyses confirm that lipid droplets are in close contact with the ER throughout various stages of cellular growth and cell division. As this interaction is very specific and presumably drives the inheritance of lipid droplets to the daughter cells, we assume that specific protein–protein or protein–lipid interactions exist that mediate this close contact.

Dynamics of lipid droplets is impaired in a seipin-deficient mutant strain

A prime candidate protein involved in mediating contacts between lipid droplets and the ER membrane is Fld1, the yeast seipin, because its absence results in an abnormal lipid droplet morphology that is also dependent on the cultivation conditions (Binns et al., 2010; Fei et al., 2008b; Szymanski et al., 2007). In our experiments, cells were cultivated either in rich medium or in SC minimal medium to stationary phase, at which time point, differences in the distribution of lipid droplets in wild-type and *fld1Δ* mutant cells are more pronounced. In accordance with previous studies (Fei et al., 2008b; Szymanski et al., 2007), *fld1Δ* mutant cells cultivated in rich medium contained one or two clusters of small to medium-sized lipid droplets. In addition, small and very small lipid droplets (<150 nm) were observed in these cells that are frequently located close to the cellular periphery. By contrast, when cells were grown in SC minimal medium, a fraction of cells contained super-sized lipid droplets instead of the rather amorphous aggregates of lipid droplets observed in *fld1Δ* cells grown in complete medium. Small lipid droplets close to the cellular periphery were also detectable, although to a lesser extent (supplementary material Fig. S9). The different morphologies of lipid droplets in cells growing in defined minimal media or complete medium is surprising. Therefore we next determined the morphological transition of lipid droplets from single super-sized lipid droplets to the fragmented clusters in more detail. Addition of complete medium to cells grown in minimal media indeed resulted in the formation of clusters of lipid droplets and the disappearance of single giant lipid droplets, indicating that giant lipid droplets formation is reversible and determined by components present in rich media. Notably, this morphological change of lipid droplets was also associated with a significant proliferation of ER membranes (Fig. 7).

In addition to the altered morphology and subcellular distribution of lipid droplets, we observed a major impact of the FLD1 deletion on the subcellular movement and inheritance of lipid droplets. Super-sized or amorphous aggregations of lipid droplets, but also medium-sized lipid droplets were significantly impaired in their delivery to the daughter cell, compared with their inheritance in wild-type cells, independently of growth conditions. In addition, we observed that lipid droplets that remained in the mother cell were not significantly degraded during several hours of cultivation (Fig. 8; supplementary material Movie 4). This impaired inheritance and degradation of lipid droplets might indeed explain their heterogeneous morphology and distribution in *fld1Δ* cell populations.

Because yeast lipid droplets always appear to be associated with ER membranes, we next studied the dynamic behavior of the ER in *fld1Δ* cells during cellular growth. It was previously observed that lipid droplets cluster along proliferated ER structures (Szymanski et al., 2007). Indeed, fluorescence 3D imaging revealed that a fraction of lipid droplets in the *fld1Δ* mutant strain was almost completely surrounded by ER membranes; super-sized lipid droplets typically appeared attached to a bar-like proliferation of the ER. Loosely clustered

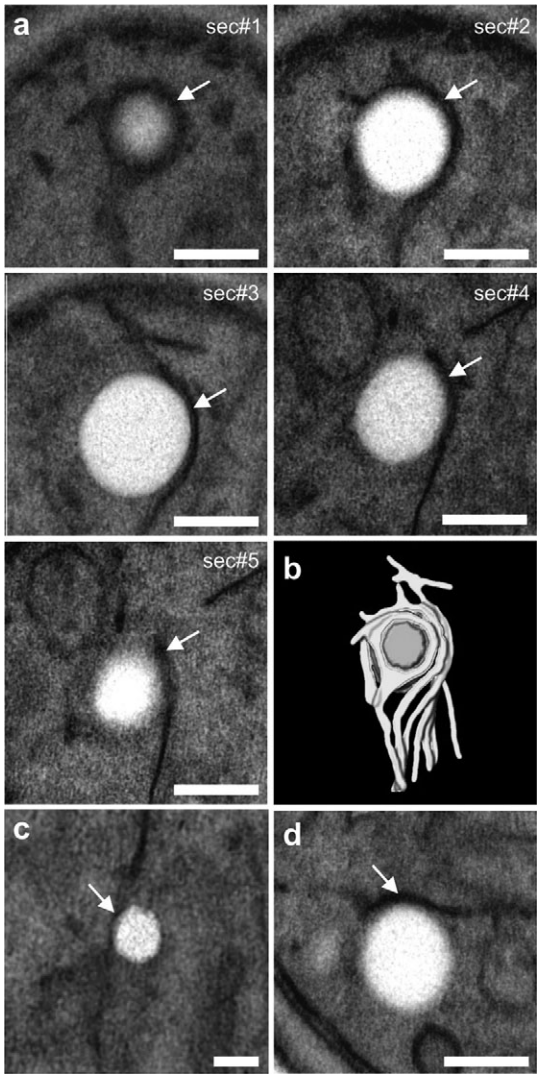

Fig. 4. Ultrastructural analysis. (**a**,**b**) Lipid-droplet–ER interactions in budding yeast cells using serial sectioning TEM. Selected region of a 3D TEM series of sections through a smaller bud. A lipid droplet close to the bud tip is partially enclosed by ER membranes (a, sec#1–sec#5; b, 3D reconstruction). Scale bars: 250 nm. (**c**) A significantly smaller lipid droplet is also attached to the ER membrane. (**d**) A lipid droplet near the bud neck is closely associated with the ER. ER tubules are indicated by arrows. Scale bars: 250 nm (a,b,d), 75 nm (c).

lipid droplets in *fld1Δ* mutant cells grown in rich medium were also surrounded by ER membranes. Electron microscopy unveiled a complex network of ER membranes in these mutants, and lipid droplets of various sizes appeared to be closely associated with these membrane structures (Fig. 9). Notably, 4D live-cell imaging of multi-labelled cells showed that these aberrant ER structures and their associated lipid droplets are not inherited and do not disappear or markedly rearrange in mother cells, during cellular growth (Fig. 10).

Lipolysis is impaired in the *fld1* mutant

In addition to the inheritance defect in the *fld1Δ* strain, 4D live-cell imaging experiments showed that the major fraction of the lipid droplets is not significantly degraded during 8 hours of cultivation. This is consistent with previously reported data that indicate an increased TAG content in the *fld1Δ* strain (Fei et al., 2008b). Lipolysis is catalyzed by Tgl3 and Tgl4 lipases, which reside on lipid droplets (Athenstaedt and Daum, 2003; Athenstaedt and Daum, 2005; Kurat et al., 2006). Therefore, we next studied whether the localization of the lipases was affected in the *fld1Δ* deletion mutant strain. In wild-type yeast cells cultivated to early stationary growth phase, Tgl3–GFP localizes to a concentrated spot on each lipid droplet (Kurat et al., 2006; Kurat et al., 2009). Within 1 hour after induction of lipolysis (addition of fresh culture medium) Tgl3–GFP redistributed to the entire surface of the lipid droplets, and remained on lipid droplets during the lipolytic and lipogenic phases of growth (Fig. 11). By contrast, Tgl3–GFP localized frequently to the entire surface of giant lipid droplets already in stationary phase in the *fld1Δ* mutant strain. Tgl3–GFP also appeared only on a subpopulation of lipid droplets in *fld1Δ* cells that contained several medium-sized lipid droplets instead of a super-sized lipid droplet. Upon supplementation with rich medium, which results in reorganization of lipid droplets as loose aggregates, Tgl3–GFP was frequently observed only on single lipid droplets, whereas neighboring lipid droplets completely lacked any GFP signal (Fig. 11). A fraction of the *fld1Δ* cell population harbored only very small lipid droplets; notably, this lipid droplet population disappeared upon stimulated lipolysis in fresh medium (supplementary material Fig. S10). Taken together, these data suggest that lipid droplet populations with different metabolic activities exist in *fld1Δ* mutants, and that Fld1 might be involved in recruiting lipid-metabolizing enzymes to the lipid droplet surface. Alternatively, access of Tgl3 lipase to the surface of lipid droplets might be impaired as a result of proliferation of the ER.

Discussion

The biology of lipid droplets has attracted great interest because of the central role of this organelle in cellular fat storage and mobilization, which are linked to prevailing metabolic disorders including obesity, type 2 diabetes and the metabolic syndrome (Farese and Walther, 2009). The use of model systems such as *Drosophila* and yeast has provided much insight into the enzymology of lipid-droplet-associated proteins and their regulation (Beller et al., 2008; Fei et al., 2008a; Guo et al., 2009; Guo et al., 2008; Szymanski et al., 2007; Walther and Farese, 2009). In this study, we have taken an imaging-based approach to understand lipid droplet motility and inheritance in yeast. We show that at least two different populations of lipid droplets might exist, which are characterized by their different subcellular dynamics in growing cells. One population of lipid droplets is dispersed towards the periphery of cells upon stimulation of growth, which is also accompanied by active lipolysis (Kurat et al., 2006). Lipid droplets that contain both TAG and steryl esters have been implicated in lipid trafficking (Daum et al., 2007), in particular to supply the plasma membrane with ergosterol that might be liberated from the lipid droplets by the plasma-membrane-resident steryl ester hydrolase Yeh2 (Koffel et al., 2005; Mullner et al., 2005). Thus it could be speculated that the two populations of lipid droplets are indeed characterized by different, specific lipid compositions, harbouring either Tag or SE. This, however, does not seem to be the case based on structural information of lipid droplets (Czabany et al., 2008) and the observation that lipid droplets in a

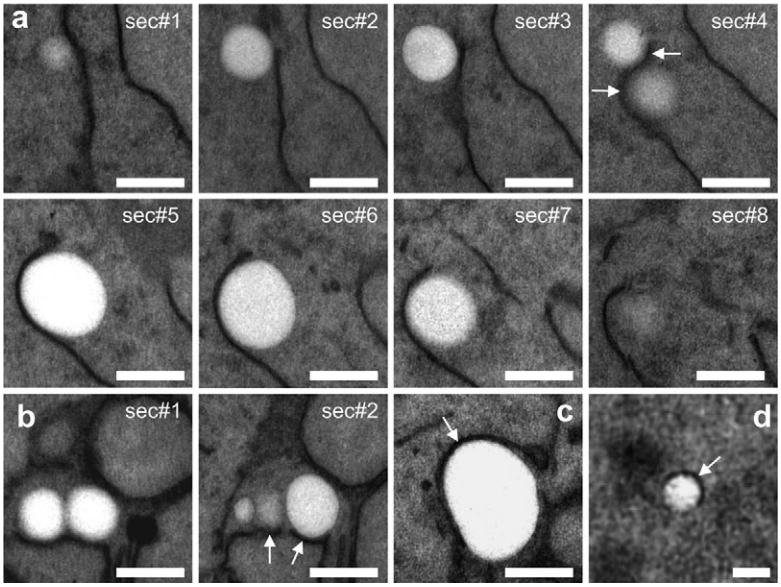

Fig. 5. Selected region of a 3D TEM series of sections through a mother cell. As in the bud, all lipid droplets in the mother cell are in close contact with ER membranes. This association is independent of the size of the lipid droplets (**a**, sec#1–8; **b**, sec#1–2; **c**,**d**). Notably, all lipid droplets appear 'embedded' in a crescent-shaped ER structure (arrows). Scale bars: 200 nm (a–c), 75 nm (d).

SE-deficient mutant (*are1Δ are2Δ*) show a comparable dispersion phenotype towards the cellular periphery during stimulated lipolysis (data not shown). Small-angle X-ray scattering of isolated lipid droplets indicates a layered structure of steryl esters below the surface of the lipid droplets and surrounding the (unordered) TAG core, and it was suggested that this lipid distribution might play an important role for the specific accessibility for lipolytic enzymes (Czabany et al., 2008). Thus, the issue of lipid droplet heterogeneity with respect to their lipid and protein content and subcellular dynamics requires further investigation.

The second population of lipid droplets is specifically targeted towards the emerging bud in growing cells, which provides the lipid supply to the daughter cells in the absence de novo fatty acid synthesis (Fig. 1). TAG lipolysis is required to drive cell cycle progression (Kurat et al., 2009), presumably to release lipid precursors for phospholipids and sphingolipids (Gaspar et al., 2011; Rajakumari et al., 2010). This supply of TAG and SE in lipid droplets from the mother cell suffices until the second daughter generation, after which cell viability rapidly decreases (supplementary material Fig. S1). What are the mechanisms that govern subcellular movement and ensure faithful lipid droplet inheritance? Lipid droplets appear to be tightly associated with ER membranes (Perktold et al., 2007; Szymanski et al., 2007), and this interaction indeed persists throughput the life cycle, bud emergence and cell division (Figs 3–6 and supplementary material S8A–C). Consequently, inheritance of lipid droplets to the daughter cells might be mediated by their attachment to the ER. It was postulated that Golgi inheritance into small buds is linked to ER inheritance (Reinke et al., 2004), which might also be the case for lipid droplets. However, ER membranes are delivered into the emerging bud in an actin-dependent matter (Fehrenbacher et al., 2002). Thus, whether there is direct contact of lipid droplets with actin or whether inheritance is mediated through the interaction of lipid droplets with ER membranes is currently unclear.

Robenek and colleagues postulated an 'egg-in-a-cup' model for lipid- droplet–ER interactions that is mediated by specific protein–protein interactions (Robenek et al., 2006). A potential candidate protein involved in mediating such an interaction in yeast is Fld1, the yeast orthologue of mammalian seipin, mutations of which are implicated in a severe inherited Seip–Berardinelli congenital lipodystrophy (Fei et al., 2008b; Szymanski et al., 2007). Yeast seipin is an oligomeric transmembrane protein that localizes to the interface between lipid droplets and the ER, and was suggested to play a role in organizing lipid droplets (Binns et al., 2010). Yeast mutants lacking Fld1 show a diverse pattern of lipid droplets in the cell population, differing in both size and subcellular distribution (Fei et al., 2008b; Szymanski et al., 2007). This striking heterogeneity of lipid droplets is also dependent on the growth medium: when grown in minimal medium, cells accumulated giant ('super-sized') lipid droplets in addition to numerous small and rather dispersed lipid droplets. By contrast, growth in complete medium led to a dispersion of the giant lipid droplets into clusters of small, but still spatially confined lipid droplets (Fig. 7; supplementary material Fig. S9). Both high-resolution fluorescence microscopy and electron microscopy revealed that lipid droplets in the *fld1Δ* mutant appear 'entangled' in a network

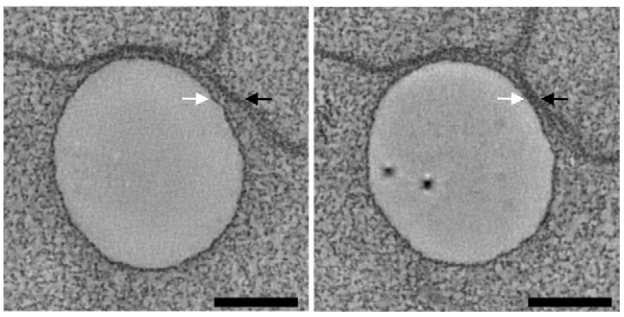

Fig. 6. Contact sites of a 'mature' lipid droplet and ER membranes. Two slices extracted from a 3D tomographic reconstruction, acquired from a yeast wild-type cell preparation. 'Gap' between the phospholipid monolayer of the lipid droplets (white arrow) and the membrane bilayer of the ER (black arrow) (left). Second slice reconstructed at a deeper layer in the specimen: here, the phospholipid monolayer of the lipid droplets is tightly associated with the ER bilayer (right). Scale bar: 50 nm.

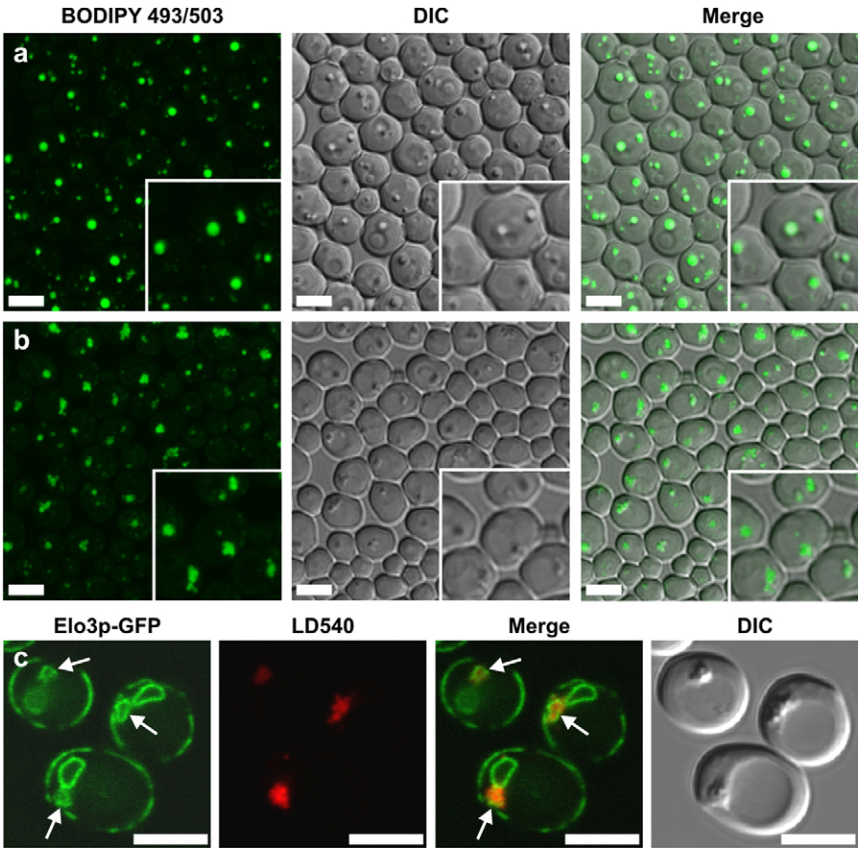

Fig. 7. Lipid droplet morphology of *fld1*Δ cells depends on growth conditions. (**a**) Cells cultivated overnight in SC medium containing super-sized lipid droplets. (**b**) Cells grown overnight in rich medium generate clusters of individual smaller lipid droplets instead of super-sized lipid droplets. (**c**) Lipid droplets clusters are adjacent to and closely associated with aberrant ER structures (arrows). Elo3–GFP-labelled ER membranes (green) and LD540-labelled lipid droplets (red). Single optical sections are shown. Scale bars: 5 µm.

of ER membranes or remain attached as super-sized lipid droplets to an unusual bar-like structure of the ER (Fig. 9). Mobility of such lipid droplets was strongly reduced compared with that of wild-type cells. The response of lipid droplets and membrane morphology to growth medium changes indicates that Fld1 might indeed play a role in ER membrane organization, which also has an impact on lipid droplet inheritance. Neither the aggregated ER structures nor the dispersed lipid droplets were transferred into the emerging daughter cells in the *fld1Δ* mutant. We conclude that the dynamics of the lipid droplets is restricted in these mutants because of their interaction with aberrant ER membranes.

The *fld1Δ* mutants are characterized by an increased TAG content (Fei et al., 2008b), which could be due to defective lipid droplet inheritance, leading to lipid accumulation in the mother cell, or a result of defective lipolysis. Because TAG degradation is dependent on Tgl3 and Tgl4 lipases on the surface of the lipid droplets (Athenstaedt and Daum, 2003; Athenstaedt and Daum, 2005; Kurat et al., 2006), we therefore investigated whether localization of the lipases was impaired in the *fld1Δ* mutant. In wild-type cells grown to stationary phase, Tgl3–GFP localizes predominantly to a small confined spot on the lipid droplet surface, and spreads upon stimulation of lipolysis over the entire lipid droplet surface (Kurat et al., 2009). By contrast, Tgl3–GFP was already homogeneously distributed over the entire surface of lipid droplets under non-inducing conditions, in *fld1Δ* mutant cells, further suggesting the Fld1 is required for organizing the lipase on the lipid droplet surface. Most surprisingly, upon appearance of dispersed lipid droplets in cells growing in SC medium, Tgl3–GFP localization was restricted to a small subpopulation of lipid droplets and was completely absent from the others. This phenomenon was particularly pronounced when *fld1Δ* cells were supplemented with rich medium, resulting in the generation of clusters of individual lipid droplets. Here, frequently only one or two lipid droplets displayed a Tgl3–GFP signal (Fig. 11). Tgl3 is presumably synthesized as a cytosolic or ER-targeted protein that is translocated to the lipid droplets by an unidentified mechanism

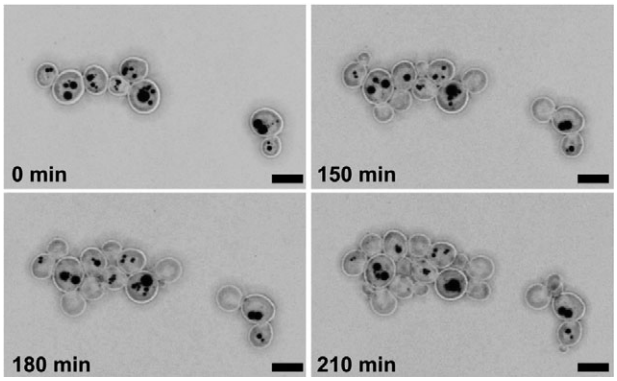

Fig. 8. Impaired dynamics of lipid droplets in the *fld1*Δ strain. 4D live-cell imaging of BODIPY493/503-labelled cells cultivated in rich medium. The inheritance of lipid droplets is significantly impaired in the deletion mutant strain. Super-sized and large lipid droplets, and also medium-sized and smaller lipid droplets are not transferred into the daughter cells. In addition, lipid droplets are not visibly degraded after several hours of cultivation. Very small lipid droplets (<150 nm) are not visualized in this medium-resolution 4D image series. Overlay of maximum-intensity projections of fluorescence data and average intensity projections of transmission. Scale bar: 5 µm.

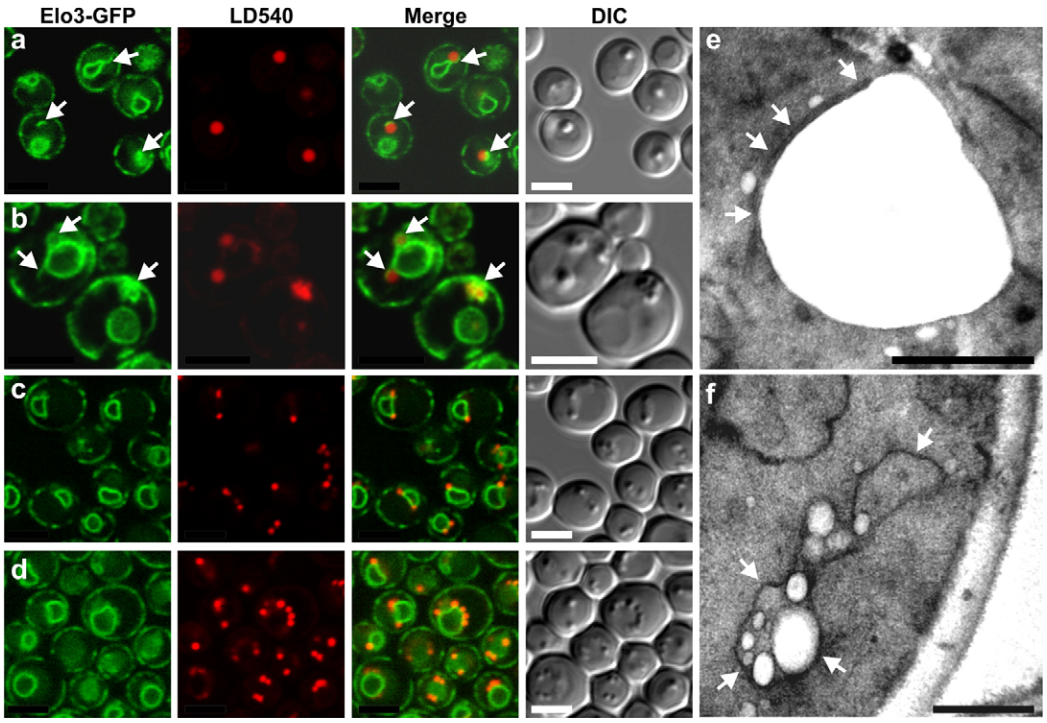

Fig. 9. Analysis of aberrant ER structures in the *fld1*Δ mutant strain cultivated in different growth media. (**a**–**f**) High-resolution images of Elo3–GFP-labelled ER (green) and LD540-labelled lipid droplets (red). Super-sized lipid droplets (cells cultivated in SC medium) are frequently attached to a short bar-like ER structure (a; e, electron micrograph, arrows). Large lipid droplets and aggregations of individual lipid droplets (cells cultivated in rich medium) are frequently enclosed by ER structures or are closely associated with a network of ER membranes (b; f, arrows). In wild-type cells, such convoluted ER structures in the vicinity of lipid droplets are not detectable. By contrast, lipid droplets are frequently associated with nuclear ER membranes (c, cell cultivated in SC medium; d, cells cultivated in rich medium). Single optical sections are shown. Scale bars: 5 µm and 500 nm (TEM images).

(Kohlwein, 2010). Thus, we propose that Fld1 is either required for sequestering Tgl3 to a specific location on the lipid droplets surface, or that access of the lipase to the lipid droplet surface is restricted because of the impaired interaction between lipid droplets and the ER membrane. Thus, both defective inheritance of lipid droplets and impaired lipolysis might contribute to the observed TAG accumulation and heterogeneous distribution of lipid droplets in the *fld1Δ* cell population.

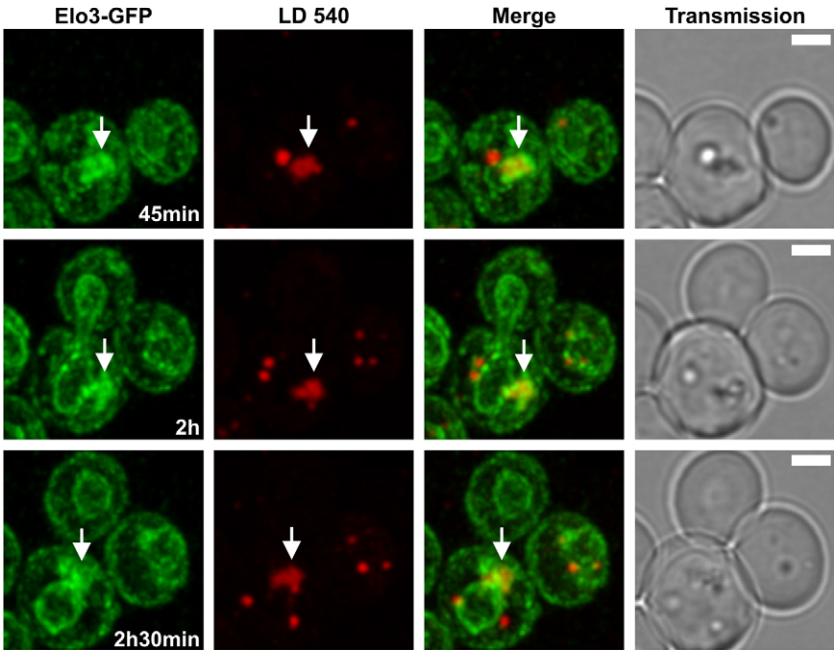

Fig. 10. Impaired dynamics of aberrant ER structures in the *fld1*Δ strain. 4D live-cell imaging of Elo3–GFP-labelled ER (green) and LD540-labelled lipid droplets (red). ER clusters and associated lipid droplets are not inherited. The abnormal ER–lipid-droplet complex is not markedly rearranged during cellular growth. Fluorescence images represent maximum-intensity projections. Transmission images represent single optical sections. Scale bars: 5 µm.

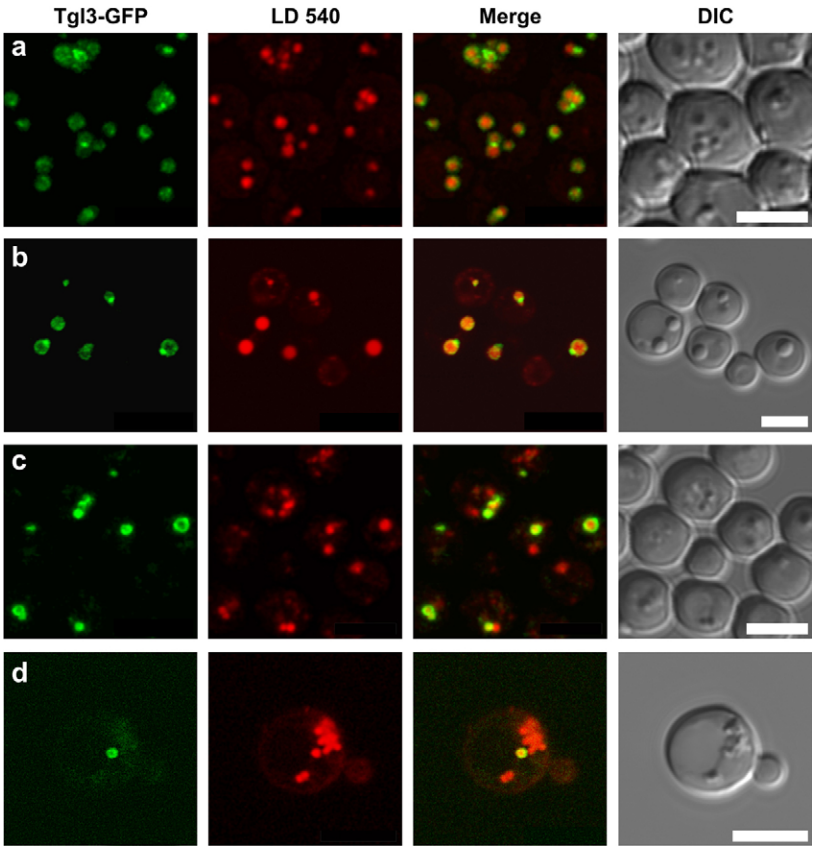

Fig. 11. Localization of the triacylglycerol lipase Tgl3 on a subpopulation of lipid droplets in the *fld1*Δ mutant strain. (**a**) In wild-type cells cultivated to stationary phase in SC medium and re-inoculated into fresh medium for 1 hour to induce lipolysis, the Tgl3–GFP signal is detected as a concentrated spot on all imaged lipid droplets and partly covering the entire surface of lipid droplets. (**b**) Under the same cultivation conditions, super-sized lipid droplets in the *fld1*Δ mutant strain show a pronounced ring-like distribution of Tgl3–GFP, in addition to one or several small Tgl3–GFP spots on the lipid droplet surface. (**c**) Subpopulation of cells cultivated in SC medium containing a few larger lipid droplets instead of single super-sized lipid droplet. Tgl3–GFP signal is seen on a subpopulation of lipid droplets. (**d**) Supplementation of *fld1*Δ cells with rich medium results in loose aggregations of lipid droplets. The Tgl3–GFP signal is detected on only one individual lipid droplet, and is absent from the other lipid droplets. Fluorescence images represent maximum-intensity projections. Transmission images represent single optical sections. Scale bars: 5 μm.

Materials and Methods

Yeast strains and growth conditions

Wild-type BY4741 (*MATa his3Δ1 lue2Δ0 met15Δ0 ura3Δ0*), single deletion mutant strain *ylr404wΔ* (*MATa his3Δ1 leu2Δ0 met15Δ0 ura3Δ0 ylr404w::KanMX4*) were obtained from EUROSCARF, Germany (Winzeler et al., 1999). The Elo3–GFP strain (BY4741 background) was obtained from Invitrogen. Yeast cells were grown at 30℃ in liquid YPD medium (1% Bacto yeast extract, 2% Bacto peptone and 2% glucose) or in liquid synthetic medium (SC medium; 0.67% nitrogen base, 2% glucose) in six-well microtiter plates (5 ml volume per well) using an Eppendorf thermomixer. Agar sheets for 4D live-cell imaging were prepared as described (Wolinski and Kohlwein, 2008). For continuous labeling of lipid droplets, the agar was supplemented with 1 μg/ml BODIPY 493/503 (Invitrogen). To block de novo synthesis of fatty acids (Omura, 1976) the agar sheets were additionally supplemented with 20 μg/ml cerulenin, as indicated (Sigma).

Fluorescence microscopy

Imaging was performed using a Leica SP5 confocal microscope and a Leica HCX 63× 1.4 NA objective. Nile Red labeling of lipid droplets and simultaneous detection of GFP and Nile Red fluorescence emission was performed as previously described (Wolinski and Kohlwein, 2008): GFP and Nile Red were both excited at 488nm; GFP fluorescence emission was detected between 500–515 nm and Nile Red fluorescence emission was detected between 560–590 nm. LD540 was a gift from Christian Thiele, Max Planck Institute of Molecular Cell Biology and Genetics, Germany (Spandl et al., 2009). LD540 labeling of lipid droplets was performed by adding the dye at a concentration of 0.5 μg/ml to the growth medium. In double-labeling experiments, GFP was excited at 488 nm and fluorescence emission was detected between 500 and 530 nm; LD540 was excited at 561 nm and fluorescence emission was detected between 570 and 600 nm.

4D live-cell imaging of yeast cells on solid agar sheets was performed with 90 × 90 × 200 nm sampling and 800 Hz scan speed. To maintain the optimal growth temperature of 30℃, the objective was heated by an objective heater system (Bioptechs). Restoration of 3D data was performed with HuygensPro 4.0 deconvolution software (Scientific Volume Imaging) and by using the classic maximum likelihood estimation algorithm (CMLE). A theoretical point spread function and five iterations were applied. Deconvolution of the slightly undersampled image stacks resulted in higher contrast of image objects than by use of Median or Gaussian filtering (Landmann, 2002). Volume rendering and image projection was performed using amira 4.0 (Visage Imaging).

Lipid droplet quantification

For estimation of the 'neutral lipid mass' in mother and daughter cells 3D image stacks of BODIPY 493/503 labelled cells were projected using the maximum-intensity projection method. Lipid droplets were segmented using manual thresholding. Finally, for each mother and daughter cell, the sum of the areas of the binarized image objects were computed. Image projection and quantification were performed using ImageJ (Girish and Vijayalakshmi, 2004).

For the determination of the number of lipid droplets in buds of different sizes yeast cells were pre-cultivated in rich medium for 72 hours to the stationary phase. Subsequently, cells were inoculated into fresh rich medium to induce bud formation, and were grown for further 90 minutes. Next, the cells were fixed with 2% formaldehyde in 50 mM Tris-HCl, pH 7.3, labelled with BODIPY 493/503 (final concentration 1 μg/ml) and imaged three-dimensionally (sampling at 90 × 90 × 240 nm). Bud sizes were determined by measuring the long axis of buds in simultaneously acquired transmission images using ImageJ. The budding index was calculated as the ratio of the longitudinal axis of the bud relative to the longitudinal axis of the mother cell. The number of lipid droplets in buds was determined interactively (two independent persons) in volume rendering projections that were generated by amira 4.0 software. At least 200 cells were analyzed in each experiment.

3D transmission electron microscopy

Cells were prepared for 3D TEM essentially as described (Waterham et al., 1994). Yeast cells were fixed with 1.5% $KMnO_4$ in distilled water for 15 minutes at room temperature, dehydrated in a graded series of ethanol (50–100%) and embedded in Epon resin. Subsequently, the specimens were polymerized for 48 hours at 60℃. Thin sections (approximately 70 nm thick) were contrasted with uranyl acetate and lead citrate. Electron microscopy was performed using a Zeiss EM 902 transmission electron microscope. Digital images were obtained using a ProScan slow scan CCD-camera.

Electron tomography

Specimens were prepared as for 3D TEM. Fiducial 10 nm Protein-A-stabilized gold particles were applied for 10 minutes on the 200-nm-thick sections. The grids were washed twice with deionised water and air-dried. Double tilt tomography series were collected on a FEI Tecnai 12 electron microscope at 120 KeV using a Fischione holder. Images were recorded on a FEI 4k × 4ks CCD Eagle camera. Tilt series were collected using 3D Explore software at a nominal magnification of

18,500× with 1.5 degree increments with the aim to cover the range between −70 to +70 degrees. Tomograms were reconstructed of the dual axes tilt series using IMOD (Kremer et al., 1996) by weighted back-projection.

Acknowledgements

The authors thank Tim van Zutphen for critically reading the manuscript and helpful suggestions.

Funding

This work was supported by grants from the Austrian Science Funds, FWF (project F3005-B12 LIPOTOX) to S.D.K. and the Austrian Federal Government for Science and Research (Project GOLD, in the framework of the Austrian Genome Program GEN-AU) to S.D.K. and H.W.

Supplementary material available online at
http://jcs.biologists.org/lookup/suppl/doi:10.1242/jcs.091454/-/DC1

References

Agarwal, A. K. and Garg, A. (2004). Seipin: a mysterious protein. *Trends Mol. Med.* **10**, 440-444.

Ashrafi, K., Chang, F. Y., Watts, J. L., Fraser, A. G., Kamath, R. S., Ahringer, J. and Ruvkun, G. (2003). Genome-wide RNAi analysis of Caenorhabditis elegans fat regulatory genes. *Nature* **421**, 268-272.

Athenstaedt, K. and Daum, G. (2003). YMR313c/TGL3 encodes a novel triacylglycerol lipase located in lipid particles of Saccharomyces cerevisiae. *J. Biol. Chem.* **278**, 23317-23323.

Athenstaedt, K. and Daum, G. (2005). Tgl4p and Tgl5p, two triacylglycerol lipases of the yeast Saccharomyces cerevisiae are localized to lipid particles. *J. Biol. Chem.* **280**, 37301-37309.

Athenstaedt, K. and Daum, G. (2006). The life cycle of neutral lipids: synthesis, storage and degradation. *Cell Mol. Life Sci.* **63**, 1355-1369.

Ayscough, K. R., Stryker, J., Pokala, N., Sanders, M., Crews, P. and Drubin, D. G. (1997). High rates of actin filament turnover in budding yeast and roles for actin in establishment and maintenance of cell polarity revealed using the actin inhibitor latrunculin-A. *J. Cell Biol.* **137**, 399-416.

Beller, M., Sztalryd, C., Southall, N., Bell, M., Jackle, H., Auld, D. S. and Oliver, B. (2008). COPI complex is a regulator of lipid homeostasis. *PLoS Biol.* **6**, e292.

Binns, D., Lee, S., Hilton, C. L., Jiang, Q. X. and Goodman, J. M. (2010). Seipin is a discrete homooligomer. *Biochemistry* **49**, 10747-10755.

Czabany, T., Wagner, A., Zweytick, D., Lohner, K., Leitner, E., Ingolic, E. and Daum, G. (2008). Structural and biochemical properties of lipid particles from the yeast Saccharomyces cerevisiae. *J. Biol. Chem.* **283**, 17065-17074.

Daum, G., Wagner, A., Czabany, T. and Athenstaedt, K. (2007). Dynamics of neutral lipid storage and mobilization in yeast. *Biochimie* **89**, 243-248.

Estrada, P., Kim, J., Coleman, J., Walker, L., Dunn, B., Takizawa, P., Novick, P. and Ferro-Novick, S. (2003). Myo4p and She3p are required for cortical ER inheritance in Saccharomyces cerevisiae. *J. Cell Biol.* **163**, 1255-1266.

Farese, R. V., Jr and Walther, T. C. (2009). Lipid droplets finally get a little R-E-S-P-E-C-T. *Cell* **139**, 855-860.

Fehrenbacher, K. L., Davis, D., Wu, M., Boldogh, I. and Pon, L. A. (2002). Endoplasmic reticulum dynamics, inheritance, and cytoskeletal interactions in budding yeast. *Mol. Biol. Cell* **13**, 854-865.

Fei, W., Alfaro, G., Muthusamy, B. P., Klaassen, Z., Graham, T. R., Yang, H. and Beh, C. T. (2008a). Genome-wide analysis of sterol-lipid storage and trafficking in Saccharomyces cerevisiae. *Eukaryot. Cell.* **7**, 401-414.

Fei, W., Shui, G., Gaeta, B., Du, X., Kuerschner, L., Li, P., Brown, A. J., Wenk, M. R., Parton, R. G. and Yang, H. (2008b). Fld1p, a functional homologue of human seipin, regulates the size of lipid droplets in yeast. *J. Cell Biol.* **180**, 473-482.

Garg, A. (2004). Acquired and inherited lipodystrophies. *N. Engl. J. Med.* **350**, 1220-1234.

Gaspar, M. L., Hofbauer, H. F., Kohlwein, S. D. and Henry, S. A. (2011). Coordination of storage lipid synthesis and membrane biogenesis: evidence for cross-talk between triacylglycerol metabolism and phosphatidylinositol synthesis. *J. Biol. Chem.* **286**, 1696-1708.

Girish, V. and Vijayalakshmi, A. (2004). Affordable image analysis using NIH Image/ImageJ. *Indian J. Cancer* **41**, 47.

Goodman, J. M. (2008). The gregarious lipid droplet. *J. Biol. Chem.* **283**, 28005-28009.

Greenspan, P., Mayer, E. P. and Fowler, S. D. (1985). Nile red: a selective fluorescent stain for intracellular lipid droplets. *J. Cell Biol.* **100**, 965-973.

Guo, Y., Walther, T. C., Rao, M., Stuurman, N., Goshima, G., Terayama, K., Wong, J. S., Vale, R. D., Walter, P. and Farese, R. V. (2008). Functional genomic screen reveals genes involved in lipid-droplet formation and utilization. *Nature* **453**, 657-661.

Guo, Y., Cordes, K. R., Farese, R. V., Jr and Walther, T. C. (2009). Lipid droplets at a glance. *J. Cell Sci.* **122**, 749-752.

Ito, D. and Suzuki, N. (2007). [Seipin/BSCL2-related motor neuron disease: Seipinopathy is a novel conformational disease associated with endoplasmic reticulum stress]. *Rinsho Shinkeigaku* **47**, 329-335.

Koffel, R., Tiwari, R., Falquet, L. and Schneiter, R. (2005). The Saccharomyces cerevisiae YLL012/YEH1, YLR020/YEH2, and TGL1 genes encode a novel family of membrane-anchored lipases that are required for steryl ester hydrolysis. *Mol. Cell Biol.* **25**, 1655-1668.

Kohlwein, S. D. (2010). Triacylglycerol homeostasis: insights from yeast. *J. Biol. Chem.* **285**, 15663-15667.

Kremer, J. R., Mastronarde, D. N. and McIntosh, J. R. (1996). Computer visualization of three-dimensional image data using IMOD. *J. Struct. Biol.* **116**, 71-76.

Kunkel, W. (1980). Effects of the antimicrotubular cancerostatic drug nocodazole on the yeast Saccharomyces cerevisiae. *Z. Allg. Mikrobiol.* **20**, 315-324.

Kurat, C. F., Natter, K., Petschnigg, J., Wolinski, H., Scheuringer, K., Scholz, H., Zimmermann, R., Leber, R., Zechner, R. and Kohlwein, S. D. (2006). Obese yeast: triglyceride lipolysis is functionally conserved from mammals to yeast. *J. Biol. Chem.* **281**, 491-500.

Kurat, C. F., Wolinski, H., Petschnigg, J., Kaluarachchi, S., Andrews, B., Natter, K. and Kohlwein, S. D. (2009). Cdk1/Cdc28-dependent activation of the major triacylglycerol lipase Tgl4 in yeast links lipolysis to cell-cycle progression. *Mol. Cell* **33**, 53-63.

Landmann, L. (2002). Deconvolution improves colocalization analysis of multiple fluorochromes in 3D confocal data sets more than filtering techniques. *J. Microsc.* **208**, 134-147.

Liu, P., Bartz, R., Zehmer, J. K., Ying, Y. S., Zhu, M., Serrero, G. and Anderson, R. G. (2007). Rab-regulated interaction of early endosomes with lipid droplets. *Biochim. Biophys. Acta.* **1773**, 784-793.

Martin, S. and Parton, R. G. (2006). Lipid droplets: a unified view of a dynamic organelle. *Nat. Rev. Mol. Cell Biol.* **7**, 373-378.

Mullner, H., Deutsch, G., Leitner, E., Ingolic, E. and Daum, G. (2005). YEH2/YLR020c encodes a novel steryl ester hydrolase of the yeast Saccharomyces cerevisiae. *J. Biol. Chem.* **280**, 13321-13328.

Omura, S. (1976). The antibiotic cerulenin, a novel tool for biochemistry as an inhibitor of fatty acid synthesis. *Bacteriol. Rev.* **40**, 681-697.

Perktold, A., Zechmann, B., Daum, G. and Zellnig, G. (2007). Organelle association visualized by three-dimensional ultrastructural imaging of the yeast cell. *FEMS Yeast Res.* **7**, 629-638.

Rajakumari, S., Rajasekharan, R. and Daum, G. (2010). Triacylglycerol lipolysis is linked to sphingolipid and phospholipid metabolism of the yeast Saccharomyces cerevisiae. *Biochim. Biophys. Acta.* **1801**, 1314-1322.

Reinke, C. A., Kozik, P. and Glick, B. S. (2004). Golgi inheritance in small buds of Saccharomyces cerevisiae is linked to endoplasmic reticulum inheritance. *Proc. Natl. Acad. Sci. USA* **101**, 18018-18023.

Robenek, H., Hofnagel, O., Buers, I., Robenek, M. J., Troyer, D. and Severs, N. J. (2006). Adipophilin-enriched domains in the ER membrane are sites of lipid droplet biogenesis. *J. Cell Sci.* **119**, 4215-4224.

Simha, V. and Garg, A. (2009). Inherited lipodystrophies and hypertriglyceridemia. *Curr. Opin. Lipidol.* **20**, 300-308.

Spandl, J., White, D. J., Peychl, J. and Thiele, C. (2009). Live cell multicolor imaging of lipid droplets with a new dye, LD540. *Traffic* **10**, 1579-1584.

Sturley, S. L. (2000). Conservation of eukaryotic sterol homeostasis: new insights from studies in budding yeast. *Biochim. Biophys. Acta.* **1529**, 155-163.

Szymanski, K. M., Binns, D., Bartz, R., Grishin, N. V., Li, W. P., Agarwal, A. K., Garg, A., Anderson, R. G. and Goodman, J. M. (2007). The lipodystrophy protein seipin is found at endoplasmic reticulum lipid droplet junctions and is important for droplet morphology. *Proc. Natl. Acad. Sci. USA* **104**, 20890-20895.

Walther, T. C. and Farese, R. V., Jr (2009). The life of lipid droplets. *Biochim. Biophys. Acta.* **1791**, 459-466.

Waterham, H. R., Titorenko, V. I., Haima, P., Cregg, J. M., Harder, W. and Veenhuis, M. (1994). The Hansenula polymorpha PER1 gene is essential for peroxisome biogenesis and encodes a peroxisomal matrix protein with both carboxy- and amino-terminal targeting signals. *J. Cell Biol.* **127**, 737-749.

Welte, M. A. (2009). Fat on the move: intracellular motion of lipid droplets. *Biochem. Soc. Trans.* **37**, 991-996.

Windpassinger, C., Auer-Grumbach, M., Irobi, J., Patel, H., Petek, E., Horl, G., Malli, R., Reed, J. A., Dierick, I., Verpoorten, N. et al. (2004). Heterozygous missense mutations in BSCL2 are associated with distal hereditary motor neuropathy and Silver syndrome. *Nat. Genet.* **36**, 271-276.

Wolinski, H. and Kohlwein, S. D. (2008). Microscopic analysis of lipid droplet metabolism and dynamics in yeast. *Methods Mol. Biol.* **457**, 151-163.

Wolinski, H., Natter, K. and Kohlwein, S. D. (2009). The fidgety yeast: focus on high-resolution live yeast cell microscopy. *Methods Mol. Biol.* **548**, 75-99.

Zanghellini, J., Natter, K., Jungreuthmayer, C., Thalhammer, A., Kurat, C. F., Gogg-Fassolter, G., Kohlwein, S. D. and von Grunberg, H. H. (2008). Quantitative modeling of triacylglycerol homeostasis in yeast–metabolic requirement for lipolysis to promote membrane lipid synthesis and cellular growth. *FEBS J.* **275**, 5552-5563.

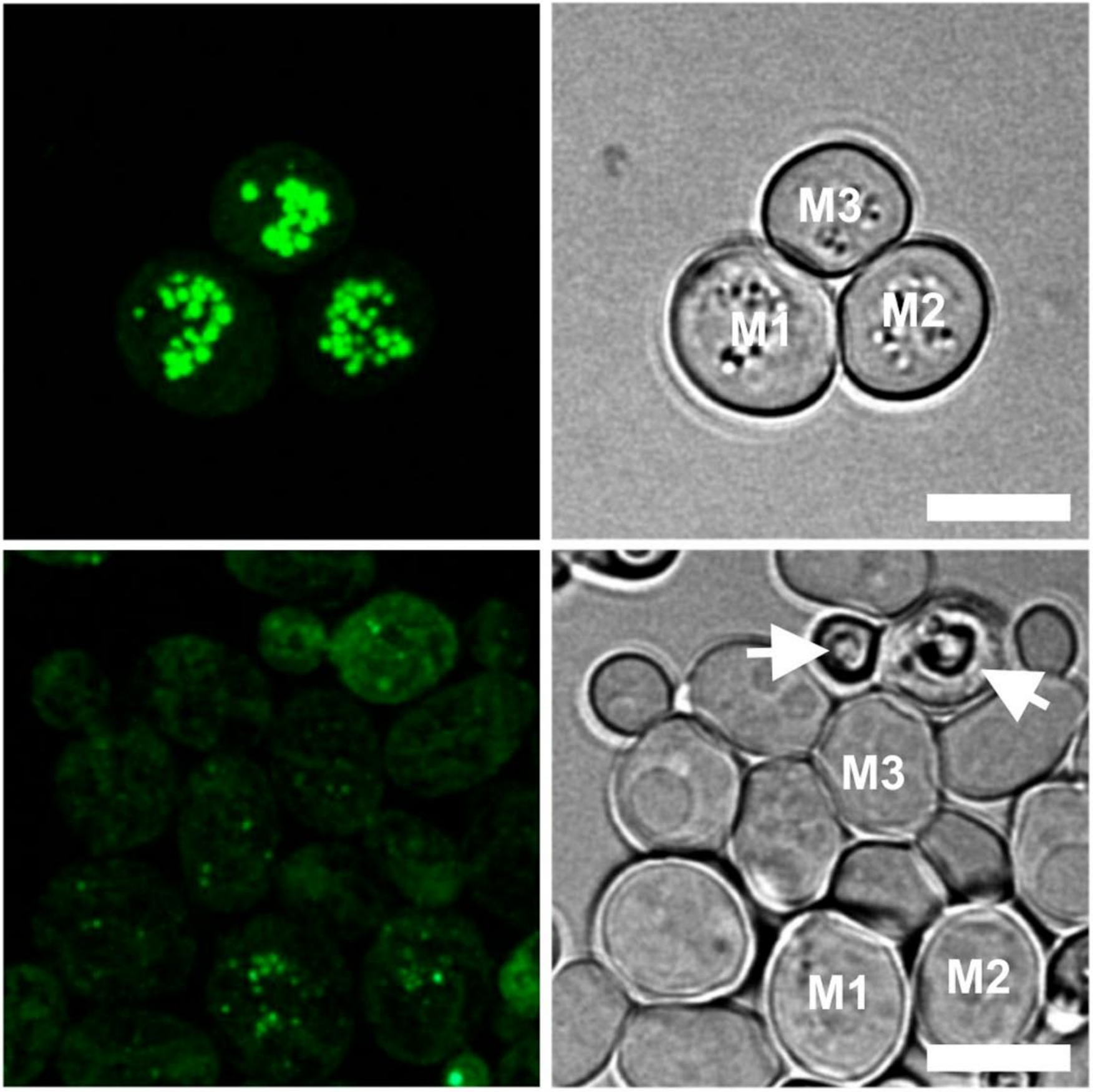
M3
M1
M2
M3
M1
M2

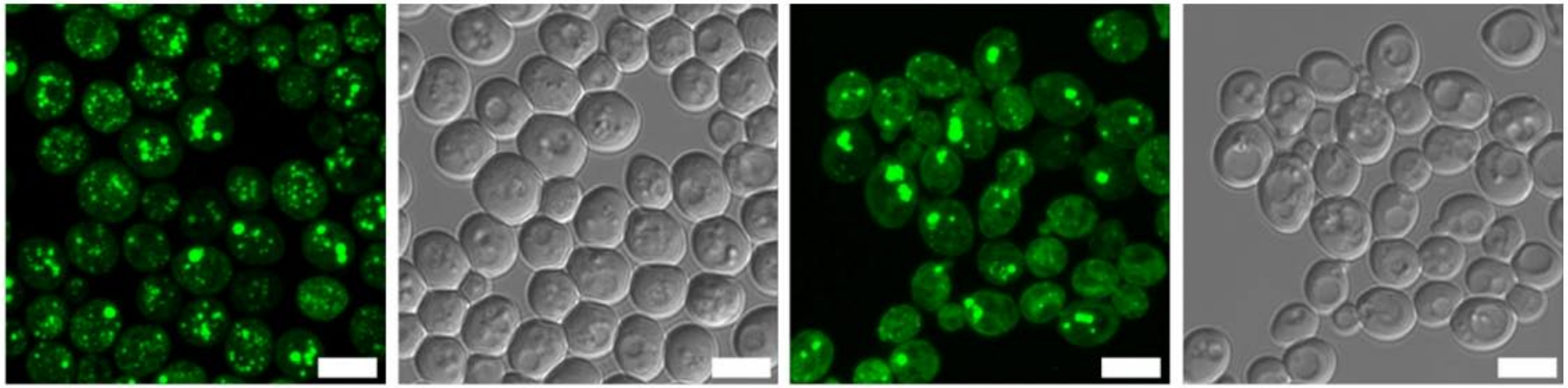

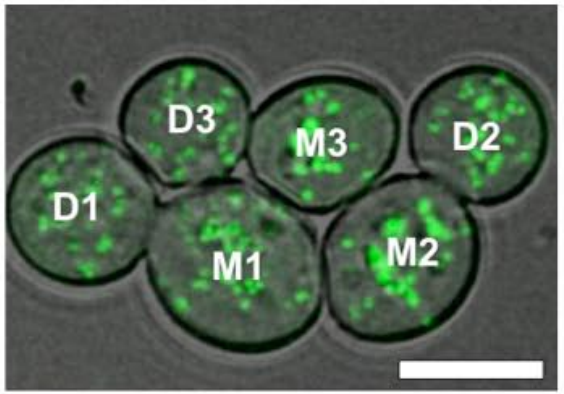
D3
M3
D2
D1
M1
M2

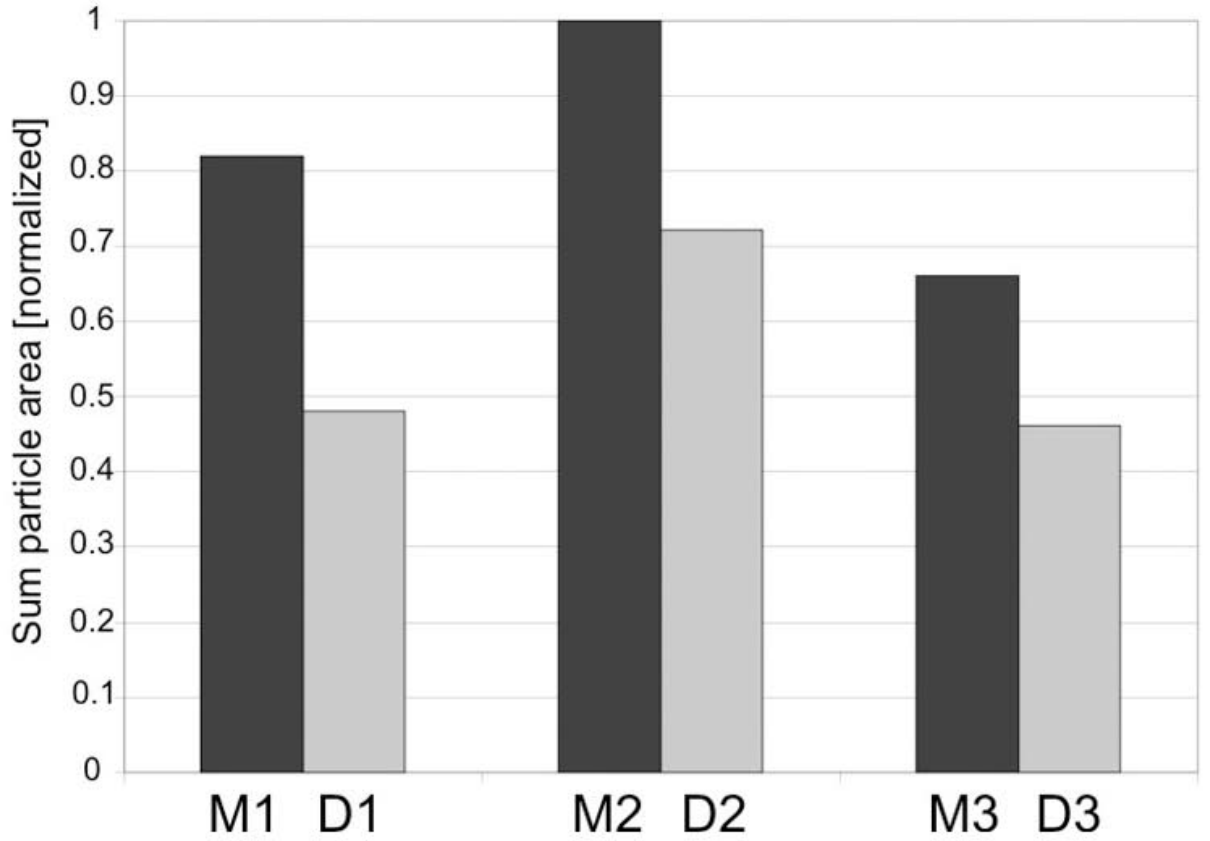
Sum particle area [normalized]
1
0.9
0.8
0.7
0.6
0.5
0.4
0.3
0.2
0.1
0
M1
D1
M2
D2
M3
D3

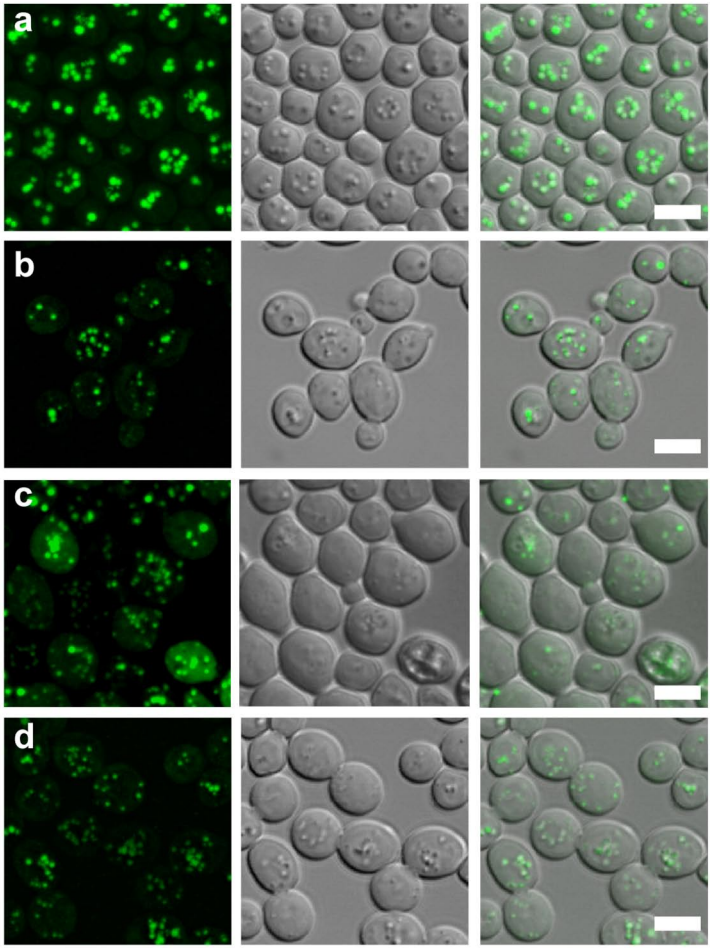
a
b
c
d

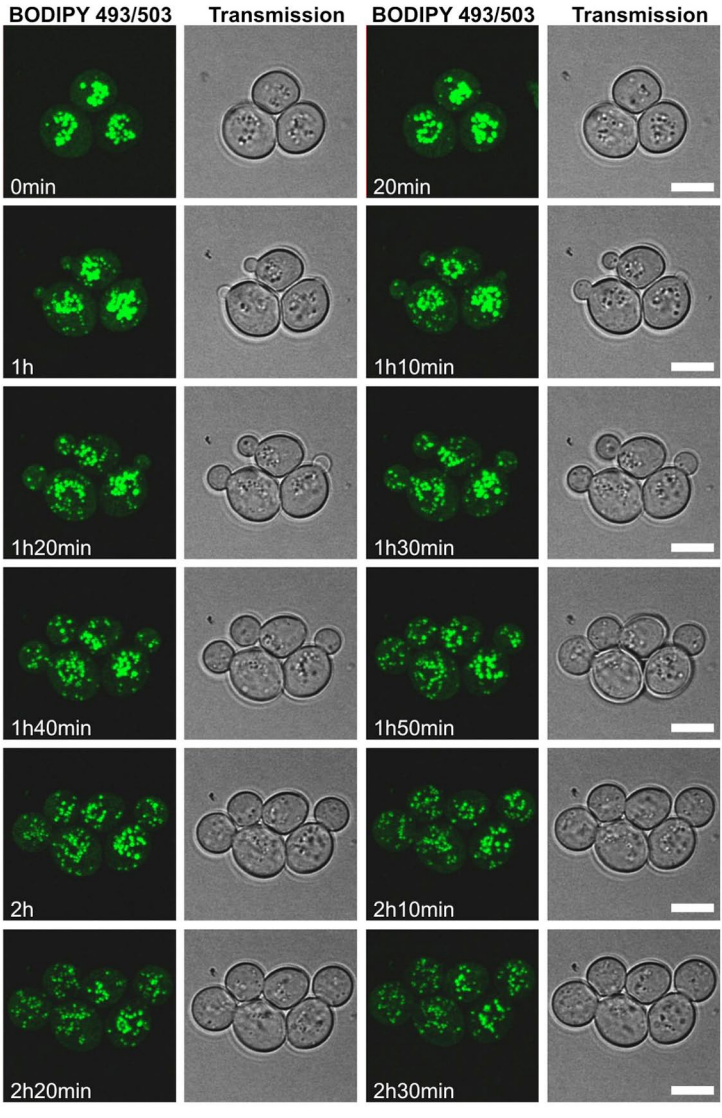
BODIPY 493/503
Transmission
BODIPY 493/503
Transmission
0min
20min
1h
1h10min
1h20min
1h30min
1h40min
1h50min
2h
2h10min
2h20min
2h30min

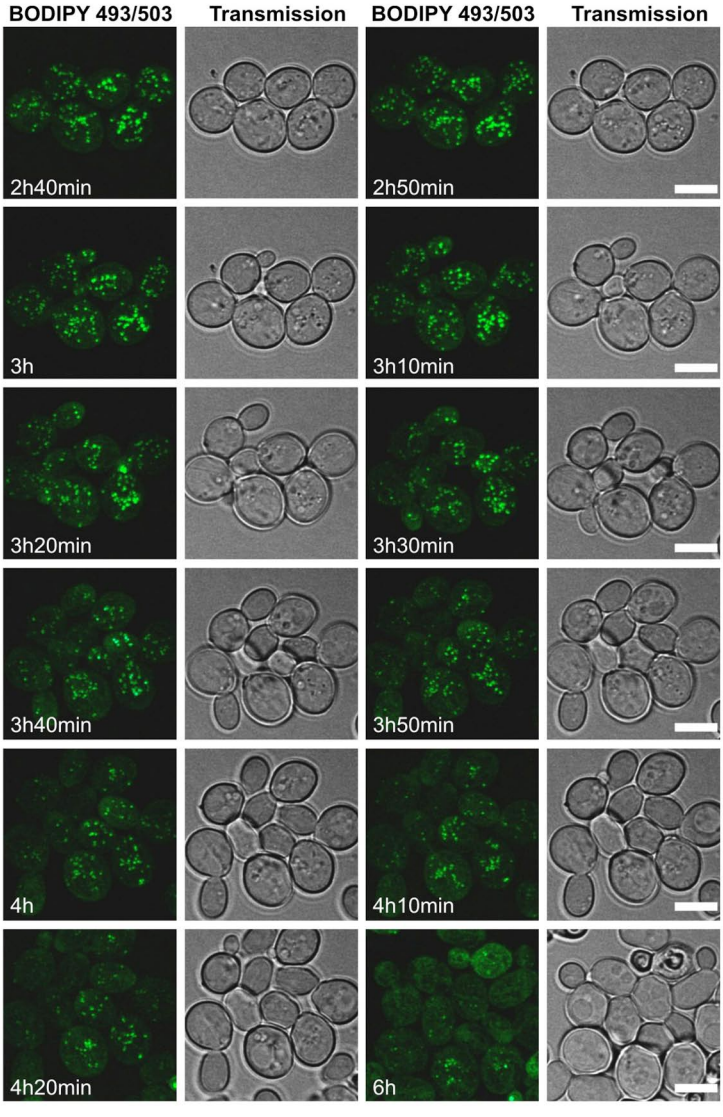
BODIPY 493/503
Transmission
BODIPY 493/503
Transmission
2h40min
2h50min
3h
3h10min
3h20min
3h30min
3h40min
3h50min
4h
4h10min
4h20min
6h

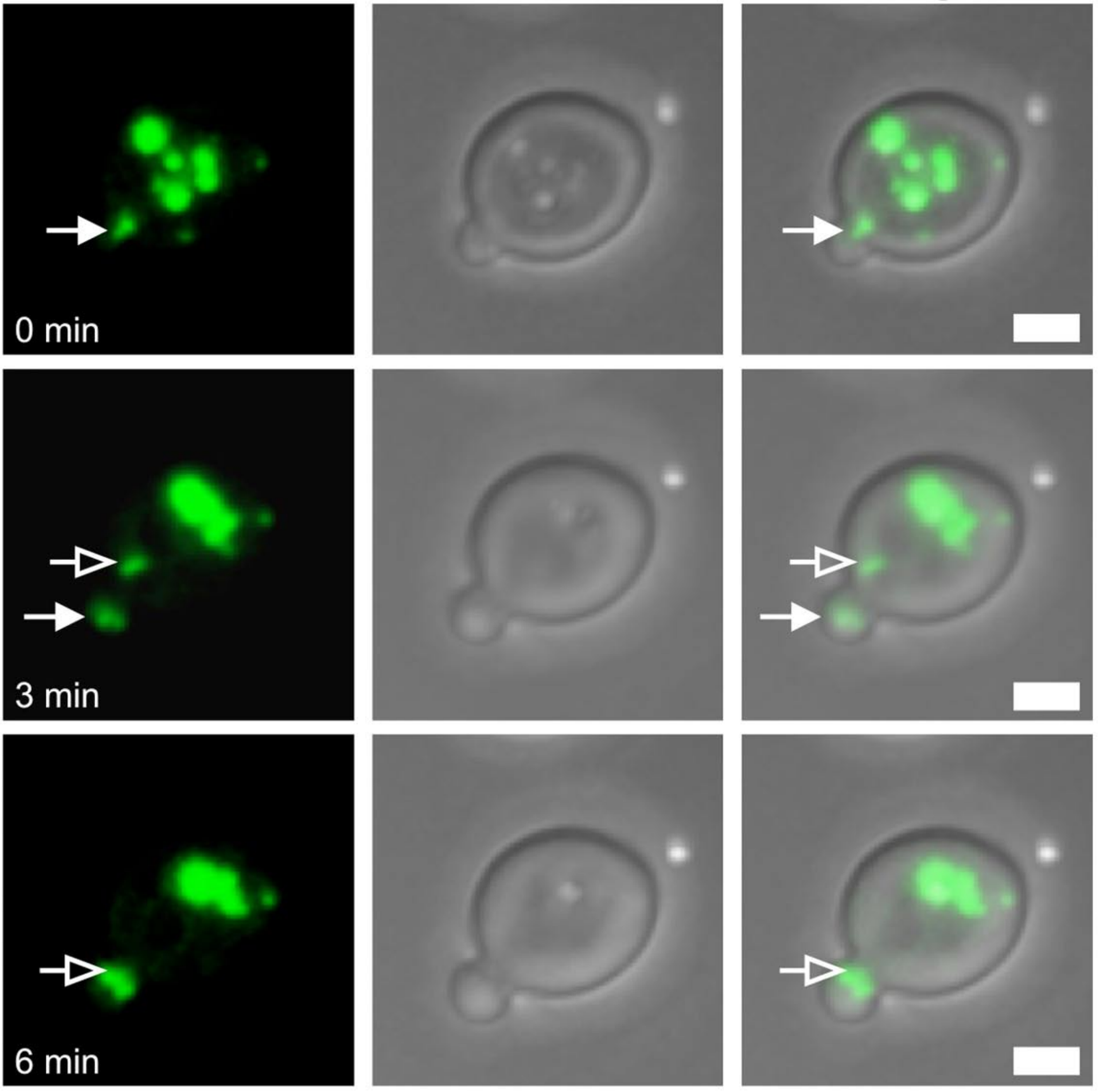
BODIPY 493/503
Transmission
Merge
0 min
3 min
6 min

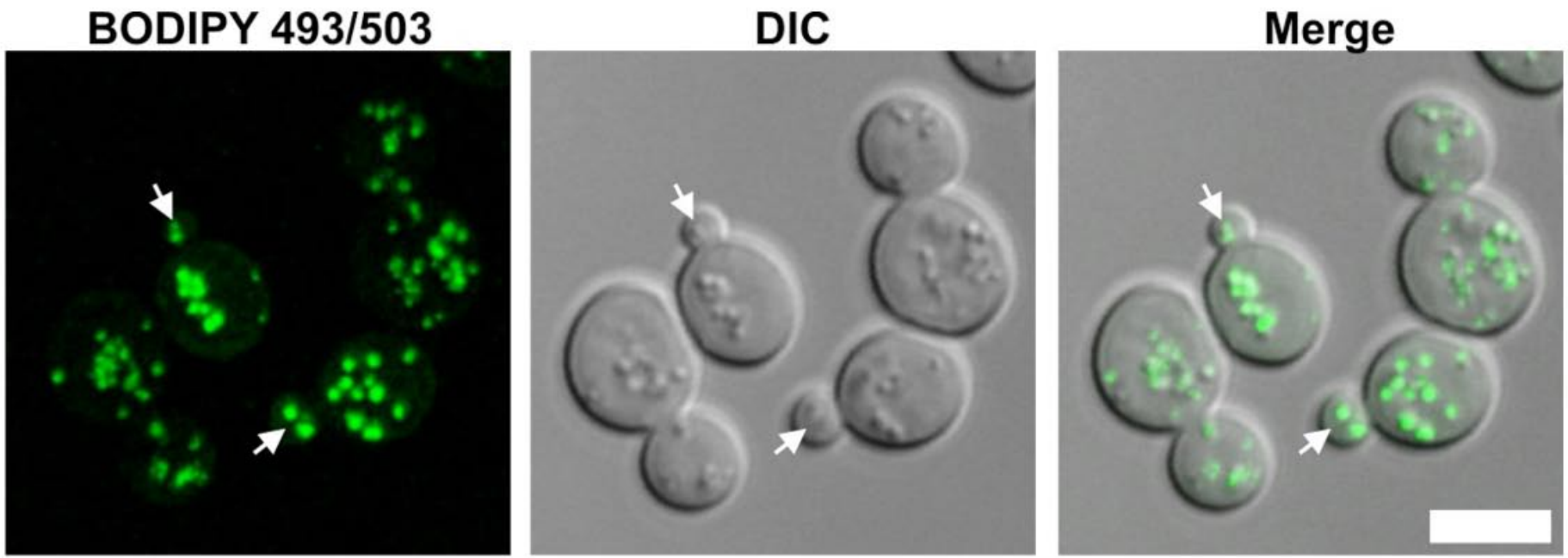
BODIPY 493/503
DIC
Merge

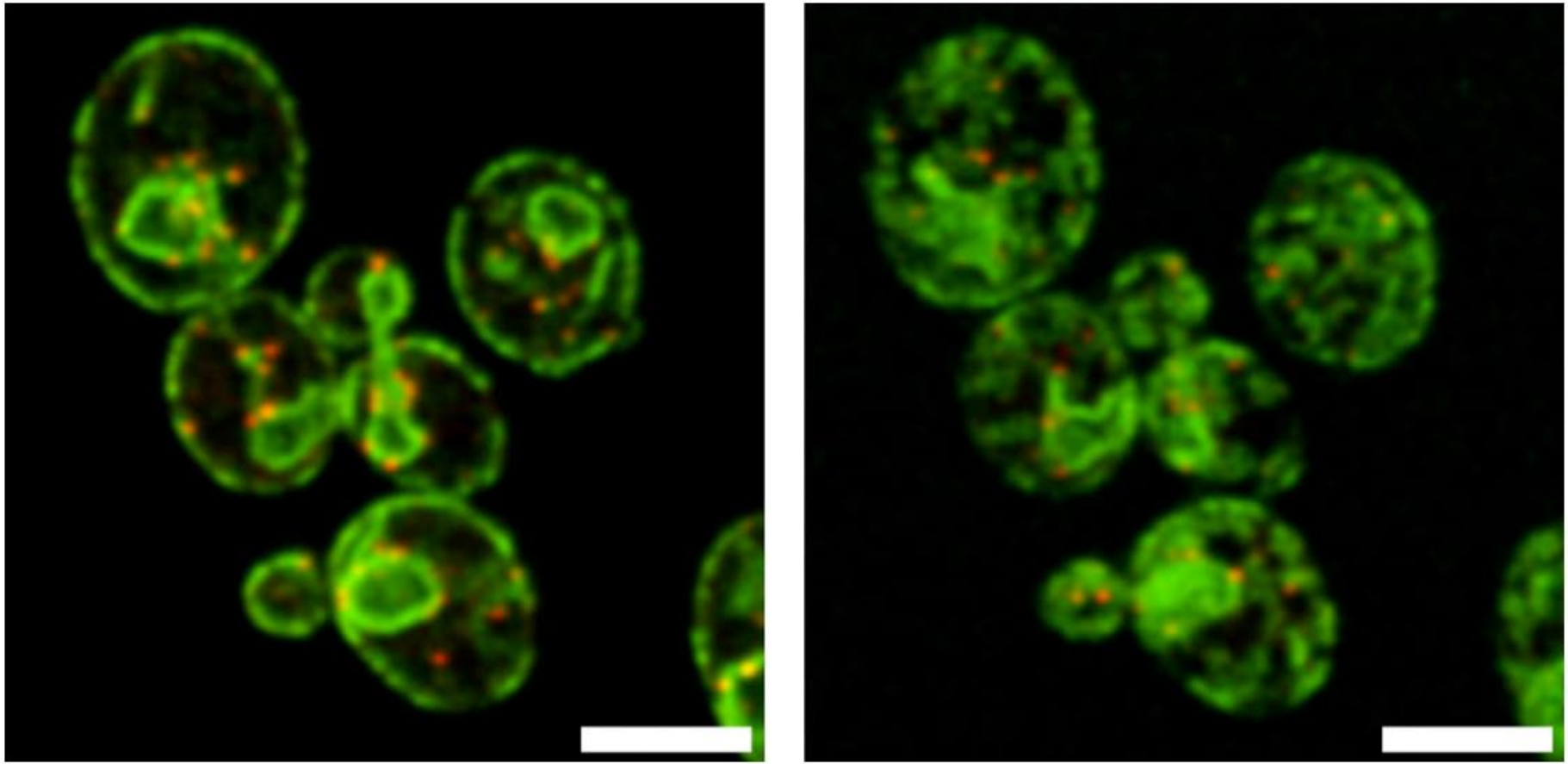

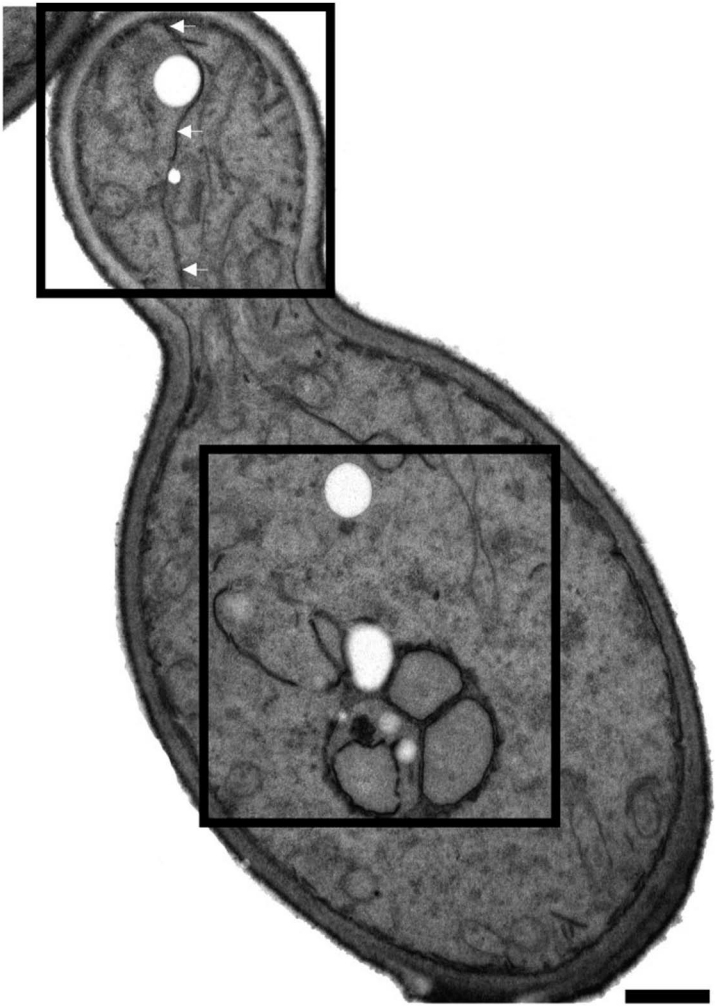

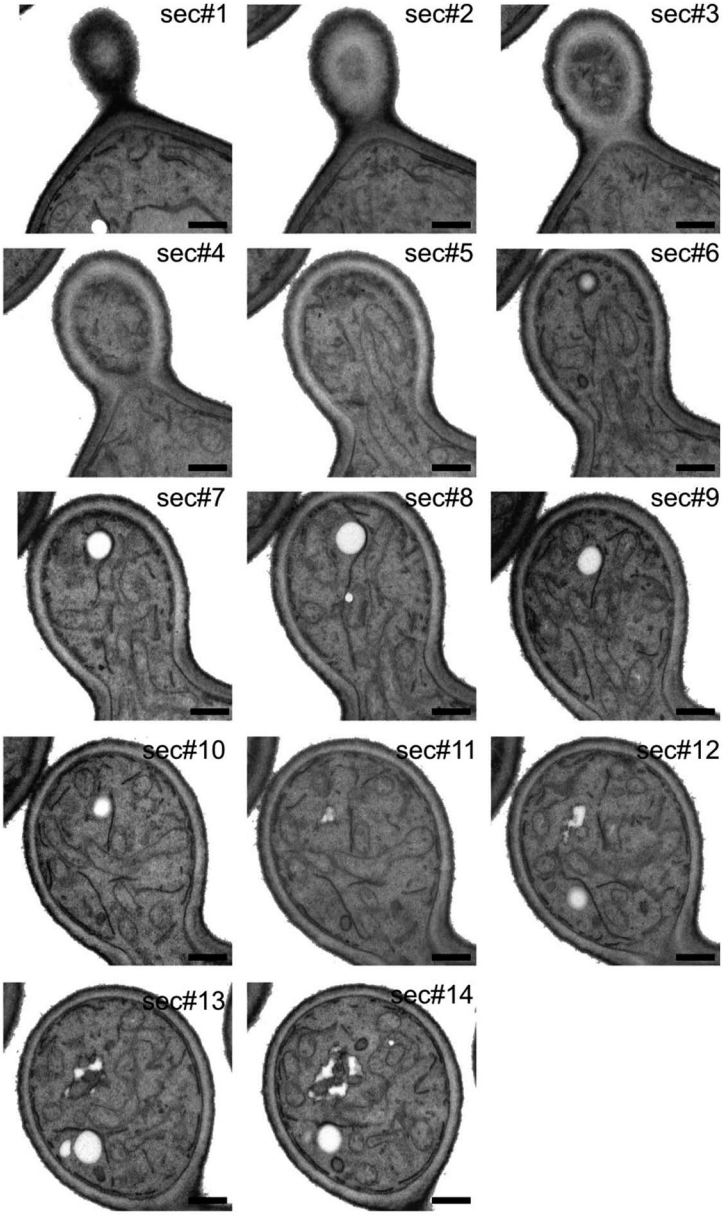
sec#1
sec#2
sec#3
sec#4
sec#5
sec#6
sec#7
sec#8
sec#9
sec#10
sec#11
sec#12
sec#13
sec#14

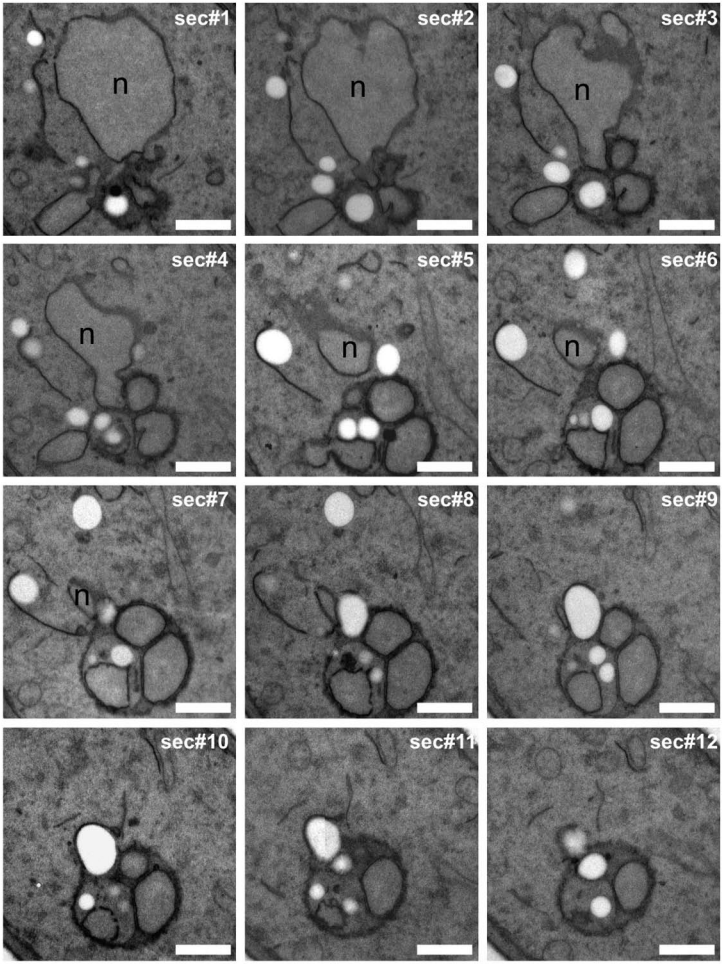
sec#1
n
sec#2
n
sec#3
n
sec#4
n
sec#5
n
sec#6
n
sec#7
n
sec#8
sec#9
sec#10
sec#11
sec#12

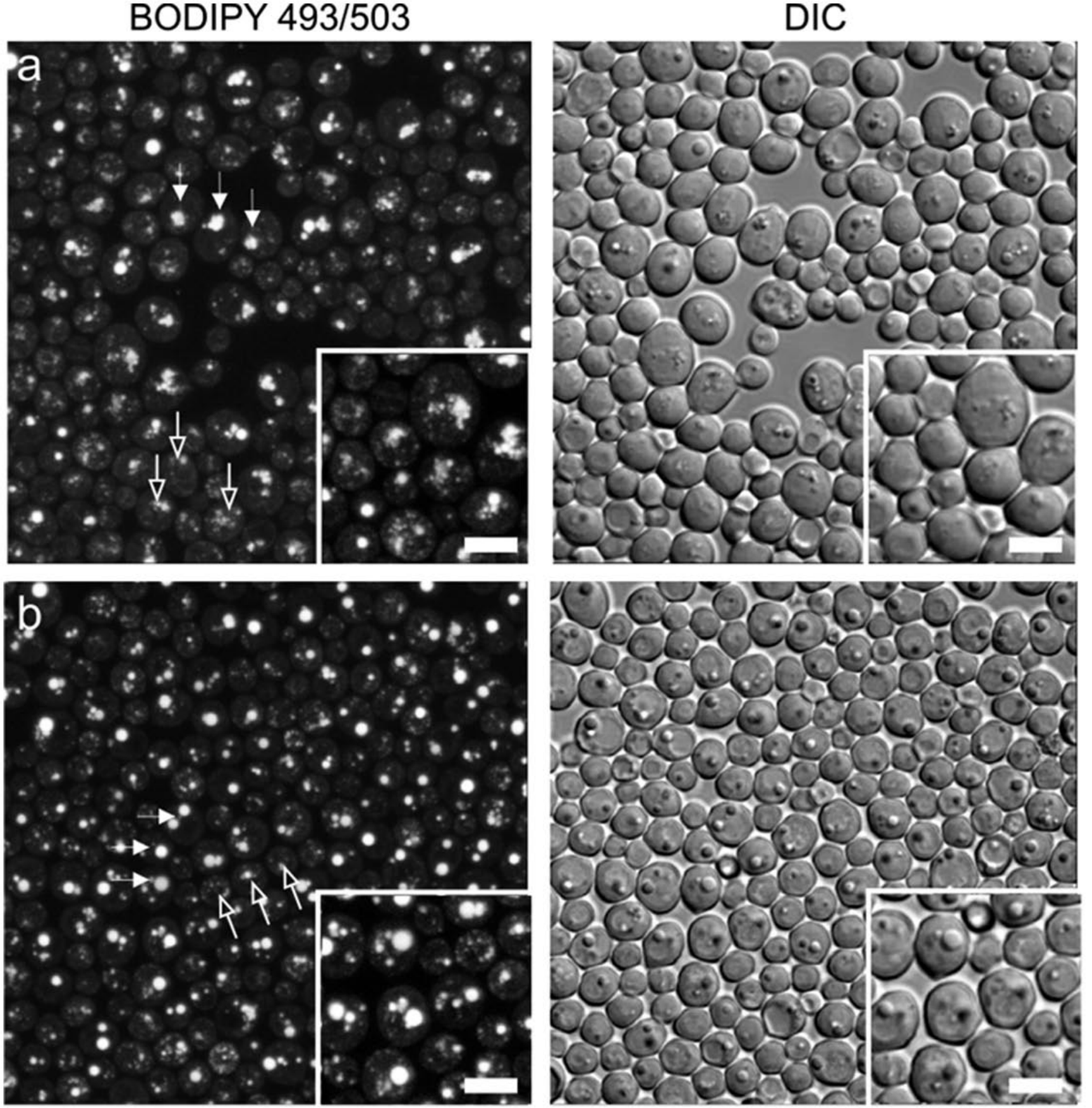
BODIPY 493/503
DIC
a
b